Using Hyperspectral Data to Identify Arctic Tundra Plant Communities and Estimate Biomass at a Low Arctic Alaska Site

Sara Nicole Bratsch
Allentown, PA

M.A. University of Texas at San Antonio, 2013
B.A. Kutztown University, 2009

A Thesis presented to the Graduate Faculty
of the University of Virginia in Candidacy for the Degree of
Master of Science

Department of Environmental Sciences

University of Virginia
May 2016

Howard Epstein
Manuel Lerdau
Jennie Moody

Abstract

Arctic ecosystems have been highly responsive to warming temperatures, with temperature increases in the Arctic occurring at rates almost twice greater than the rest of the globe over the past few decades. Changes to arctic ecosystems include increased albedo and surface heat flux, longer and warmer growing seasons, altered patterns of precipitation and evapotranspiration, decreased snow cover, and increased soil temperature and permafrost thaw. These factors result in vegetation changes such as increased vascular plant coverage, change in species composition, increased shrub coverage, and greater vegetation biomass in the Low Arctic, a region where plant vegetation communities have been historically dominated by mosses and lichens. Remote sensing is a useful tool for tracking these vegetation changes. This is commonly done using broad-band indices such as Normalized Difference Vegetation Index (NDVI), which has been used to identify a 9-15% increase in greenness in the Alaskan Arctic from 1982-2010. However, many changes to Arctic vegetation systems are occurring on a species level where differences may not be identifiable with broad-band remote sensing. Despite this, the use of hyperspectral remote sensing for assessing vegetation dynamics remains scarce.

This study uses handheld hyperspectral remote sensing data collected during the 1999 growing season to establish relationships between spectra and vegetation communities and vegetation community biomass and to show how hyperspectral remote sensing methods can improve upon traditional methods for arctic vegetation community classification and biomass estimation. In Chapter 1, I assess the ability of hyperspectral data to differentiate among four vegetation communities in the Low Arctic of Alaska. Ivotuk, Alaska, serves as my primary study site. I then use models from Ivotuk to predict community membership at five other research sites along the North Slope of Alaska. Results show high accuracy when differentiating communities

within the Ivotuk site, and mixed accuracy at the other sites. Sites located nearer to Ivotuk have better community differentiation while more northern sites had decreased classification accuracy. In Chapter 2, I use hyperspectral data and harvested biomass data to develop relationships between spectra and biomass quantities for plant tissue types at Ivotuk, Alaska. Biomass-spectra relationships were most significant for shrubs and shrub component parts, supporting other findings that shrubs are dominant controls over reflectance in arctic vegetation communities.

This research finds that hyperspectral remote sensing is a valuable tool for identifying vegetation communities and tracking biomass changes occurring with climate change. Both chapters suggest that regions outside of typical NDVI, specifically bands in the blue, green, and red edge, may contain more useful information for differentiating among communities and estimating biomass. Hyperspectral remote sensing is therefore a valuable tool for Arctic research as it allows us to identify finer differences in vegetation communities. This study presents an example of the use of hyperspectral remote sensing to improve upon classification of tundra vegetation communities in the Arctic. Research sites in Alaska are remote and accessing sites is expensive. Ground-based remote sensing studies are crucial as they allow for the development of spectral relationships that can then potentially be extrapolated to hyperspectral satellite remote sensing, and used to track vegetation changes on larger temporal and spatial scales.

Acknowledgements

I would first like to thank my advisor, Howie Epstein, for his support and guidance throughout the completion of my Master's thesis, and for taking a chance on me at a time of great educational change in my life. I would also like to thank my other committee members, Manuel Lerdau and Jennie Moody, for their support throughout the development of this thesis. I would like to thank various people at the University of Virginia including fellow members of the Epstein lab Itiya Aneece and Jeff Atkins, and Heather Landes for her help on various aspects of this research. I would like to thank the National Fish and Wildlife Foundation and the Department of Environmental Sciences at UVA for funding my research. Fieldwork at Ivotuk was conducted as part of the Arctic Transitions in the Land-Atmosphere System (ATLAS) project (NSF OPP-9908829). This data analysis was funded as part of the NASA Pre-ABoVE (Arctic Boreal Vulnerability Experiment) project (Grant NNX13AM20G). Fieldwork for the Dalton Highway sites was conducted as part of the hy-ARC-VEG (hyperspectral method development for ARCtic VEGetation biomes). I would like to thank Marcel Buchhorn for the use of data collected during the hy-ARC-VEG project as test data for models developed at Ivotuk.

I am thankful to my friends and family for their support throughout this process and throughout my entire educational experience. I would like to thank my high school English teacher, Thomas Wilde, for unknowingly setting me upon this educational journey back in his 3rd floor classroom in the Annex at Allen. I would like to thank my boyfriend, Nathan Heep, for standing beside me while I took this leap into a new career field and to a new state. Finally, I would like to thank my parents and my sister for their support throughout my education and my life, and for instilling in me a love of education from an early age, without which none of this would have been possible.

Table of Contents

List of Tables

List of Figures

Introduction

Arctic ecosystems have warmed at greater rates than the rest of the globe through a process known as polar amplification (Serreze and Francis 2006, Winton 2006, Walker et al. 2012), with global change in temperature estimated to be 0.17°C per decade (Hansen et al. 2010) and warming in the Arctic (>64°N) estimated at 0.60 ± 0.07°C per decade (Comiso and Hall 2014). This has been associated with reduction in sea-ice extent and changes to surface albedo (Kaufman et al. 2009, Comiso and Hall 2014). Arctic ecosystems have been highly responsive to climate change (Epstein et al. 2004a, Raynolds et al. 2008a, Jia et al. 2009, Zeng et al. 2011, Hinzman et al. 2013), resulting in changes to albedo, surface heat fluxes, a decrease in temperature seasonality (Xu et al. 2013), changes in precipitation and evapotranspiration (New et al. 2001, Huemmrich et al. 2010b), an increase in permafrost thaw (Walker et al. 2003b, Hinzman et al. 2013, Saito et al. 2013), a decrease in snow cover (Saito et al. 2013), and an increase in soil temperatures (Ueyama et al. 2013, Williamson et al. 2014).

Temperature changes have been linked to a lengthening of the growing season (Huemmrich et al. 2010b, Zeng et al. 2011), an increase in shrub cover (Sturm et al. 2001a, Sturm et al. 2001b, Tape et al. 2006, Myers-Smith et al. 2011), and an average increase in Alaskan tundra biomass of 7.8% from 1982-2010 (Epstein et al. 2012). Warming trends have led to increases in vascular plant coverage in Low Arctic ecosystems traditionally dominated by mosses and lichens (Huemmrich et al. 2013). The observed increases in shrub abundance may be due to their ability to outcompete low-lying vegetation, potentially through shading of non-vascular species (Chapin et al. 1995, Cornelissen et al. 2001, Sturm et al. 2001a).

Changes to vegetation biomass and greenness have been examined using greenness indices such as the Normalized Difference Vegetation Index (NDVI) (e.g. Jia and Epstein 2003,

Stow et al. 2004, Riedel et al. 2005a, Raynolds et al. 2006, Jia et al. 2009), with an observed 9-15% increase in NDVI across the North American Arctic from 1982-2010 (Bhatt et al. 2010, Raynolds et al. 2012). Past studies have mapped changes in vegetation using aerial photography (Sturm et al. 2005), coarse-scale satellite imagery such as that from the Advanced Very High Resolution Radiometer (AVHRR) (Walker 1999), and moderate-scale satellite imagery such as that from Landsat platforms (Muller et al. 1999, Silapaswan et al. 2001). Though vegetation change in the Arctic occurs on fine spatial scales, the use of high-resolution imagery remains scarce (however, see Forbes et al. 2010, Buchhorn et al. 2013, Huemmrich et al. 2013).

While past studies have been integral for mapping vegetation on a pan-Arctic scale, finer-scale studies are needed to better understand changes in tundra plant functional types (PFTs) and vegetation communities (Stow et al. 2004). Hyperspectral remote sensing provides a potential avenue through which these changes can be better tracked and analyzed. Huemmrich et al. (2013) call for research on spectral properties to distinguish among physiological characteristics of shrubs and other arctic vegetation types. This thesis explores the use of hyperspectral remote sensing to identify differences among tundra vegetation communities and to quantify plant biomass.

I conducted my study using hand-held hyperspectral data collected from Ivotuk, Alaska (68.49°N, 155.74°W) during the 1999 growing season. Ivotuk is located along the North Slope of the Brooks Mountain Range (Epstein et al. 2004b, Riedel et al. 2005a, Riedel et al. 2005b), and is largely a tussock tundra ecosystem that is also dominated by deciduous shrubs (Walker et al. 2003a). The four plant communities in this study—moist acidic tundra (MAT), moist nonacidic tundra (MNT), moss tundra (MT), and shrub tundra (ST)—all occur within a 2 km^2 area at Ivotuk (Riedel et al. 2005a).

In Chapter 1, I use hyperspectral data to differentiate among four different vegetation communities (MAT, MNT, MT, ST) during both early and peak growing season. I define the spectral signatures of these four plant communities at Ivotuk, Alaska and then use this information to predict the presence of these communities at five other sites along the Dalton Highway, on the North Slope of Alaska (Figure 1.1). I identify the average spectral signature for each vegetation community and use a combination sparse partial least squares-discriminant analysis method to identify the most significant hyperspectral narrowbands (HNBs) for differentiating among communities.

In Chapter 2, I examine the relationship between spectra and aboveground biomass quantities for the various plant functional types and tissue types at Ivotuk, Alaska. I use LASSO regression to establish relationships between biomass quantities and hyperspectral data during early and peak growing season. I create relationships using all vegetation communities in aggregate, and then again to create unique relationships within vegetation communities.

Remote sensing allows scientists to monitor vegetation changes occurring at a variety of spatial and temporal scales. Identifying the fine-scale differences in vegetation communities will allow us to track changes in vegetation composition and biomass quantities resulting from climate change. Fieldwork in Alaska is expensive and logistically difficult. Remotely tracking of vegetation changes in the Arctic will allow us to gather much larger amounts of information. This thesis seeks to develop relationships between hyperspectral data and vegetation communities and their component parts that can then be applied to other sites in the Alaskan Arctic and potentially scaled to hyperspectral satellites and used to estimate vegetation composition, biomass quantities, and to track vegetation changes in arctic ecosystems.

References

Bhatt, U. S., D. A. Walker, M. K. Raynolds, J. C. Comiso, H. E. Epstein, G. Jia, R. Gens, J. E. Pinzon, C. J. Tucker, C. E. Tweedie, and P. J. Webber. 2010. Circumpolar Arctic Tundra Vegetation Change Is Linked to Sea Ice Decline. Earth Interactions **14**:1-20.

Buchhorn, M., D. Walker, B. Heim, M. Raynolds, H. Epstein, and M. Schwieder. 2013. Ground-Based Hyperspectral Characterization of Alaska Tundra Vegetation along Environmental Gradients. Remote Sensing **5**:3971-4005.

Chapin, F. S., G. R. Shaver, A. E. Giblin, K. J. Nadelhoffer, and J. A. Laundre. 1995. Responses of Arctic Tundra to Experimental and Observed Changes in Climate. Ecology **76**:694-711.

Comiso, J. C., and D. K. Hall. 2014. Climate trends in the Arctic as observed from space. Wiley Interdisciplinary Reviews: Climate Change **5**:389-409.

Cornelissen, J. H., T. V. Callaghan, J. M. Alatalo, A. Michelsen, E. Graglia, A. E. Hartley, D. Hik, S. E. Hobbie, M. C. Press, C. H. Robinson, G. H. Henry, G. R. Shaver, G. K. Phoenix, D. Gwynn Jones, S. Jonasson, F. S. Chapin III, U. Molau, C. Neill, J. A. Lee, J. M. Melillo, B. Sveinjörnsson, and R. Aerts. 2001. Global change and arctic ecosystems: is lichen decline a function of increases in vascular plant biomass? Journal of Ecology **89**:984-994.

Epstein, H. E., J. Beringer, W. A. Gould, A. H. Lloyd, C. D. Thompson, F. S. Chapin III, G. J. Michaelson, C. L. Ping, T. S. Rupp, and D. A. Walker. 2004a. The nature of spatial transitions in the Arctic. Journal of Biogeography **31**:1917-1933.

Epstein, H. E., M. P. Calef, M. D. Walker, F. S. Chapin III, and A. M. Starfield. 2004b. Detecting changes in arctic tundra plant communities in response to warming over decadal time scales. Global Change Biology **10**:1325-1334.

Epstein, H. E., M. K. Raynolds, D. A. Walker, U. S. Bhatt, C. J. Tucker, and J. E. Pinzon. 2012. Dynamics of aboveground phytomass of the circumpolar Arctic tundra during the past three decades. Environmental Research Letters **7**:015506.

Forbes, B. C., M. M. Fauria, and P. Zetterberg. 2010. Russian Arctic warming and 'greening' are closely tracked by tundra shrub willows. Global Change Biology **16**:1542-1554.

Hansen, J., R. Ruedy, M. Sato, and K. Lo. 2010. Global Surface Temperature Change. Reviews of Geophysics **48**.

Hinzman, L. D., C. J. Deal, A. D. McGuire, S. H. Mernild, I. V. Polyakov, and J. E. Walsh. 2013. Trajectory of the Arctic as an integrated system. Ecological Applications **23**:1837-1868.

Huemmrich, F., J. A. Gamon, C. E. Tweedie, P. Campbell, D. R. Landis, and E. Middleton. 2013. Arctic Tundra Vegetation Functional Types Based on Photosynthetic Physiology and Optical Properties. IEEE Journal of Selected Topics in Applied Earth Observations and Remote Sensing **6**:265-275.

Huemmrich, K. F., G. Kinoshita, J. A. Gamon, S. Houston, H. Kwon, and W. C. Oechel. 2010. Tundra carbon balance under varying temperature and moisture regimes. Journal of Geophysical Research **115**.

Jia, G. J., and H. E. Epstein. 2003. Greening of arctic Alaska, 1981–2001. Geophysical Research Letters **30**.

Jia, G. J., H. E. Epstein, and D. A. Walker. 2009. Vegetation greening in the Canadian Arctic related to decadal warming. J Environ Monit **11**:2231-2238.

Kaufman, D. S., D. P. Schneider, N. P. McKay, C. M. Ammann, R. S. Bradley, K. R. Briffa, G. H. Miller, B. L. Otto-Bliesner, J. T. Overpeck, B. M. Vinther, and M. Arctic Lakes 2k Project. 2009. Recent warming reverses long-term arctic cooling. Science **325**:1236-1239.

Muller, S. V., A. E. Racoviteanu, and D. A. Walker. 1999. Landsat MSS-derived land-cover map of northern Alaska: extrapolation methods and a comparison with photo-interpreted and AVHRR-derived maps. International Journal of Remote Sensing **20**:2921-2946.

Myers-Smith, I. H., B. C. Forbes, M. Wilmking, M. Hallinger, T. Lantz, D. Blok, K. D. Tape, M. Macias-Fauria, U. Sass-Klaassen, E. Lévesque, S. Boudreau, P. Ropars, L. Hermanutz, A. Trant, L. S. Collier, S. Weijers, J. Rozema, S. A. Rayback, N. M. Schmidt, G. Schaepman-Strub, S. Wipf, C. Rixen, C. B. Ménard, S. Venn, S. Goetz, L. Andreu-Hayles, S. Elmendorf, V. Ravolainen, J. Welker, P. Grogan, H. E. Epstein, and D. S. Hik. 2011. Shrub expansion in tundra ecosystems: dynamics, impacts and research priorities. Environmental Research Letters **6**:045509.

New, M., M. Todd, M. Hulme, and P. Jones. 2001. Precipitation measurements and trends in the twentieth century. International Journal of Climatology **21**:1889-1922.

Raynolds, M., J. Comiso, D. Walker, and D. Verbyla. 2008. Relationship between satellite-derived land surface temperatures, arctic vegetation types, and NDVI. Remote Sensing of Environment **112**:1884-1894.

Raynolds, M. K., D. A. Walker, H. E. Epstein, J. E. Pinzon, and C. J. Tucker. 2012. A new estimate of tundra-biome phytomass from trans-Arctic field data and AVHRR NDVI. Remote Sensing Letters **3**:403-411.

Raynolds, M. K., D. A. Walker, and H. A. Maier. 2006. NDVI patterns and phytomass distribution in the circumpolar Arctic. Remote Sensing of Environment **102**:271-281.

Riedel, S., H. E. Epstein, D. A. Walker, D. L. Richardson, M. P. Calef, E. Edwards, and A. Moody. 2005a. Spatial and Temporal Heterogeneity of Vegetation Properties among Four Tundra Plant Communities at Ivotuk, Alaska, U. S. A. Arctic, Antarctic, and Alpine Research **37**:25-33.

Riedel, S. M., H. E. Epstein, and D. A. Walker. 2005b. Biotic controls over spectral reflectance of arctic tundra vegetation. International Journal of Remote Sensing **26**:2391-2405.

Saito, K., T. Zhang, D. Yang, S. Marchenko, R. G. Barry, V. Romanovsky, and L. Hinzman. 2013. Influence of the physical terrestrial Arctic in the eco-climate system. Ecological Applications **23**:1778-1797.

Serreze, M. C., and J. A. Francis. 2006. The Arctic Amplification Debate. Climatic Change **76**:241-264.

Silapaswan, C., D. Verbyla, and A. D. McGuire. 2001. Land Cover Change on the Seward Peninsula: The Use of Remote Sensing to Evaluate the Potential Influences of Climate Warming on Historical Vegetation Dynamics. Canadian Journal of Remote Sensing **27**:542-554.

Stow, D. A., A. Hope, D. McGuire, D. Verbyla, J. Gamon, F. Huemmrich, S. Houston, C. Racine, M. Sturm, K. Tape, L. Hinzman, K. Yoshikawa, C. Tweedie, B. Noyle, C. Silapaswan, D. Douglas, B. Griffith, G. Jia, H. Epstein, D. Walker, S. Daeschner, A. Petersen, L. Zhou, and R. Myneni. 2004. Remote sensing of vegetation and land-cover change in Arctic Tundra Ecosystems. Remote Sensing of Environment **89**:281-308.

Sturm, M., J. P. McFadden, G. E. Liston, F. S. Chapin III, C. Racine, and J. Holmgren. 2001a. Snow-Shrub Interactions in Arctic Tundra: A Hypothesis with Climate Implications. Journal of Climate **14**:336-344.

Sturm, M., C. Racine, and K. D. Tape. 2001b. Increasing shrub abundance in the Arctic. Nature **411**:1251-1256.

Sturm, M., J. P. Schimel, G. J. Michaelson, J. M. Welker, S. F. Oberbauer, G. E. Liston, J. Fahnestock, and V. E. Romanovsky. 2005. Winter Biological Processes Could Help Convert Arctic Tundra to Shrubland. BioScience **55**:17-26.

Tape, K. E. N., M. Sturm, and C. Racine. 2006. The evidence for shrub expansion in Northern Alaska and the Pan-Arctic. Global Change Biology **12**:686-702.

Ueyama, M., K. Iwata, Y. Harazono, E. S. Euskirchen, W. C. Oechel, and D. Zona. 2013. Growing season and spatial variations of carbon fluxes of Arctic and boreal ecosystems in Alaska (USA). Ecological Applications **23**:1798-1816.

Walker, D. A. 1999. An integrated vegetation mapping approach for northern Alaska (1:4 M scale). International Journal of Remote Sensing **20**:2895-2920.

Walker, D. A., H. E. Epstein, G. Jia, A. Balser, C. Copass, E. J. Edwards, W. A. Gould, J. Hollingsworth, J. A. Knudson, H. A. Maier, A. Moody, and M. K. Raynolds. 2003a. Phytomass, LAI, and NDVI in northern Alaska: Relationships to summer warmth, soil pH, plant functional types, and extrapolation to the circumpolar Arctic. Journal of Geophysical Research **108**.

Walker, D. A., H. E. Epstein, M. K. Raynolds, P. Kuss, M. A. Kopecky, G. V. Frost, F. J. A. Daniëls, M. O. Leibman, N. G. Moskalenko, G. V. Matyshak, O. V. Khitun, A. V. Khomutov, B. C. Forbes, U. S. Bhatt, A. N. Kade, C. M. Vonlanthen, and L. Tichý. 2012. Environment, vegetation and greenness (NDVI) along the North America and Eurasia Arctic transects. Environmental Research Letters **7**:015504.

Walker, D. A., G. J. Jia, H. E. Epstein, M. K. Raynolds, F. S. Chapin Iii, C. Copass, L. D. Hinzman, J. A. Knudson, H. A. Maier, G. J. Michaelson, F. Nelson, C. L. Ping, V. E. Romanovsky, and N. Shiklomanov. 2003b. Vegetation-soil-thaw-depth relationships along a low-arctic bioclimate gradient, Alaska: synthesis of information from the ATLAS studies. Permafrost and Periglacial Processes **14**:103-123.

Williamson, S., D. Hik, J. Gamon, J. Kavanaugh, and G. Flowers. 2014. Estimating Temperature Fields from MODIS Land Surface Temperature and Air Temperature Observations in a Sub-Arctic Alpine Environment. Remote Sensing **6**:946-963.

Winton, M. 2006. Amplified Arctic climate change: What does surface albedo feedback have to do with it? Geophysical Research Letters **33**.

Xu, L., R. B. Myneni, F. S. Chapin Iii, T. V. Callaghan, J. E. Pinzon, C. J. Tucker, Z. Zhu, J. Bi, P. Ciais, H. Tømmervik, E. S. Euskirchen, B. C. Forbes, S. L. Piao, B. T. Anderson, S. Ganguly, R. R. Nemani, S. J. Goetz, P. S. A. Beck, A. G. Bunn, C. Cao, and J. C. Stroeve. 2013. Temperature and vegetation seasonality diminishment over northern lands. Nature Climate Change.

Zeng, H., G. Jia, and H. Epstein. 2011. Recent changes in phenology over the northern high latitudes detected from multi-satellite data. Environmental Research Letters **6**:045508.

Chapter 1: Differentiating among Four Arctic Tundra Plant Communities at Ivotuk, Alaska Using Field Spectroscopy

1. Abstract

Warming in the Arctic has resulted in changes in the distribution and composition of vegetation communities. Many of these changes are occurring at fine spatial scales and at the level of individual species. Broad-band, coarse-scale remote sensing methods are commonly used to assess vegetation changes in the Arctic, and may not be appropriate for detecting these fine-scale changes; however, the use of hyperspectral, high resolution data for assessing vegetation dynamics remains scarce. The aim of this chapter is to assess the ability of field spectroscopy to differentiate among four vegetation communities in the Low Arctic of Alaska. Primary data were collected from the North Slope site of Ivotuk, Alaska (68.49°N, 155.74°W) and analyzed using spectrally resampled hyperspectral narrowbands (HNBs). A two-step sparse partial least squares (SPLS) and linear discriminant analysis (LDA) was used for community separation. Results from Ivotuk were then used to predict community membership at five other sites along the Dalton Highway in Arctic Alaska. Overall classification accuracy at Ivotuk ranged from 84%–94% and from 55%–91% for the Dalton Highway test sites. The results of this study suggest that hyperspectral data acquired at the field level, along with the SPLS and LDA methodology, can be used to successfully discriminate among Arctic tundra vegetation communities in Alaska, and present an improvement over broad-band, coarse-scale methods for community classification.

2. Introduction

Remote sensing has allowed for the assessment of changes occurring in arctic vegetation at a variety of spatial and temporal scales (Stow et al. 2004). Past studies have mapped vegetation changes at high northern latitudes using aerial photography (Sturm et al. 2005), coarse-scale satellite imagery such as that from the Advanced Very High Resolution Radiometer (AVHRR) (Walker 1999), and moderate-scale satellite imagery such as that from Landsat platforms (Muller et al. 1999, Silapaswan et al. 2001). The Normalized Difference Vegetation Index (NDVI), a remotely sensed indicator of photosynthetic capacity (Tucker 1979), is one of the most commonly used spectral vegetation indices (SVIs), and is widely available from satellite sensors, such as the AVHRR, the Moderate-Resolution Imaging Spectroradiometer (MODIS), and the various Landsat sensors that capture spectral information in a few broad spectral bands. NDVI provides an accessible means to monitor changes in the quantity of green vegetation on broad spatial and relatively long temporal scales. NDVI is therefore frequently used to evaluate vegetation changes in high latitude environments (Tucker 1979, Hope et al. 1993, Vierling et al. 1997, Walker et al. 2003a, Stow et al. 2004, Riedel et al. 2005b, Olthof and Latifovic 2007, Laidler et al. 2008, Huemmrich et al. 2010a, Huemmrich et al. 2010b, Myers-Smith et al. 2011, Epstein et al. 2012). One of the previous analyses at the site of interest for this study (Ivotuk, Alaska) showed that, at the landscape scale, broad-band NDVI obtained by averaging hyperspectral bands across red and near infrared (NIR) regions had the greatest peak growing season values for shrub tundra (ST), compared to three other tundra plant communities (Riedel et al. 2005a). While NDVI may be useful for separating some communities at peak growing season, it may be problematic during the early or late growing season when vegetation communities are more similar (Figure 1.1). Broad-band NDVI is calculated from two coarse regions of the

spectrum (Tucker 1979), which can potentially obscure important information in spectra that might be useful for differentiating among vegetation communities.

Vegetation changes in the Arctic are likely occurring at fine spatial and spectral scales and at the level of individual species, the monitoring of which may benefit from the use of hyperspectral remote sensing (Buchhorn et al. 2013). More defined regions of the visible and near infrared spectra than those captured by multispectral sensors, including those outside the range of NDVI bands, can be used to identify functional and structural properties of vegetation communities (Curran 1989, Ustin and Gamon 2010). Tundra vegetation communities are often comprised of bare soils or large quantities of non-vascular components (mosses and lichens) that affect the spectral signatures of vegetation communities (Hope et al. 1993, Vogelmann and Moss 1993). Ground-based remote sensing data have been collected from a variety of sites throughout the North Slope of Alaska (Huemmrich et al. 2010a, Boelman et al. 2011, Walker et al. 2012, Buchhorn et al. 2013, Huemmrich et al. 2013); this hyperspectral remote sensing (also known as imaging spectroscopy) information has been useful in differentiating among distinct vegetation communities in the Arctic (Buchhorn et al. 2013), as well as between vascular and non-vascular vegetation (Huemmrich et al. 2013). A discriminant analysis of peak season data from Barrow, Alaska, found moss and vascular plant spectra to have similar reflectances in the green and NIR wavelengths, while lichens had higher reflectance in the visible wavelengths and greater variability among species-specific reflectances (Huemmrich et al. 2013). Dead biomass in the Arctic also influences NDVI and reflectivity spectra. This factor becomes more influential as shrubs begin to dominate these systems, and their leaf litter covers more low-lying plants (DeMarco et al. 2014, Xu et al. 2014).

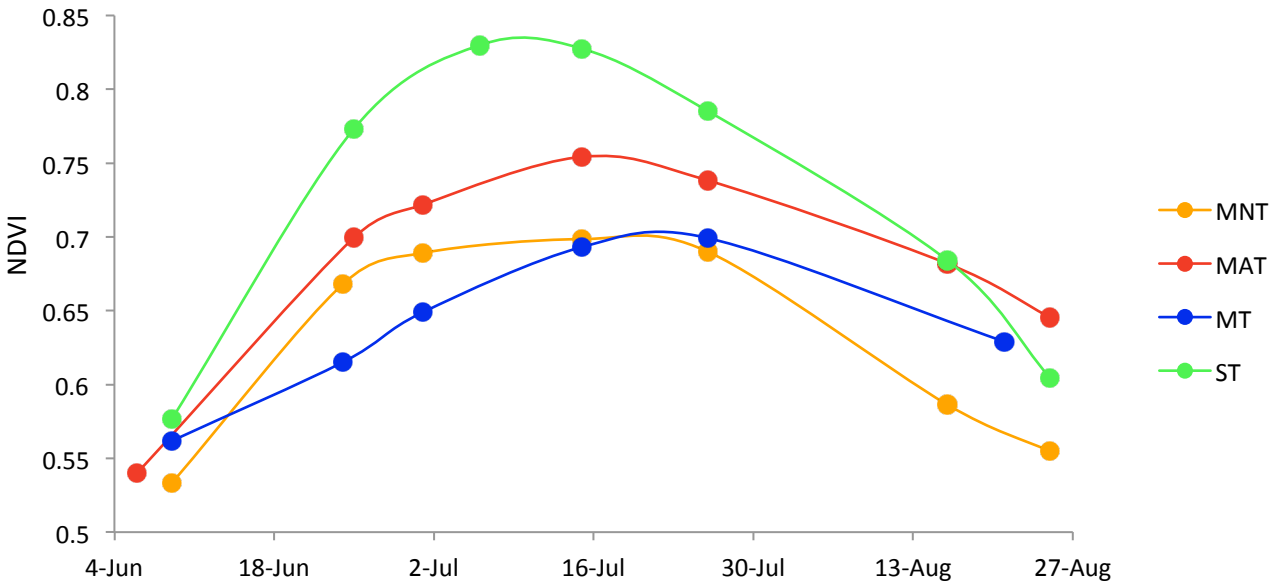

Figure 1.1 NDVI throughout the 1999 growing season for four different vegetation communities at Ivotuk, Alaska. Adapted from (Riedel et al. 2005a). Measurements were taken using an Analytical Spectral Devices FieldSpec spectro-radiometer.

The objective of this chapter is to differentiate among Alaskan Arctic tundra plant communities through the use of field spectroscopy and to identify diagnostic wavelength regions for discriminating among these communities at different phenological stages. Ivotuk, Alaska is first used to develop a model for identifying different vegetation communities using hyperspectral data; this discrimination model is then applied to five other sites on the North Slope of Alaska to test its utility in identifying tundra vegetation across geographical space.

3. Materials and Methods

3.1 Arctic Change

The Arctic has warmed at a greater rate than the rest of the globe through a process known as polar amplification (Serreze and Francis 2006, Winton 2006, Walker et al. 2012). This warming phenomenon is largely attributed to a reduction in sea-ice extent and concomitant changes in albedo (Kaufman et al. 2009, Comiso and Hall 2014). From 1981–2012, the change in global temperature was observed to be ~0.17 °C per decade (Hansen et al. 2010), while warming in the Arctic (>66°N) was approximately 0.60 ± 0.07 °C per decade (Comiso and Hall 2014). Satellite observations from 1982–2008 have shown greater warming trends in the North American Arctic (+30%) than in the Eurasian Arctic (+16%) based on the Summer Warmth Index (SWI), which is defined as the sum of average monthly surface temperatures above freezing (Bhatt et al. 2010). Temperature changes have likely caused a lengthening of the growing season in the Arctic (Huemmrich et al. 2010b, Zeng et al. 2011), and associated vegetation changes such as greater vegetation biomass (Jia et al. 2004, Bhatt et al. 2010, Epstein et al. 2012, Hinzman et al. 2013), changes in vegetation composition and leaf area index (LAI) (Elmendorf et al. 2012), and an increase in shrub cover (Sturm et al. 2001a, Sturm et al. 2001b, Tape et al. 2006, Myers-Smith et al. 2011). Vegetation greenness as determined by the NDVI has increased approximately 9% in the North American Arctic, while greenness in the Eurasian Arctic has increased by only 2% since 1982 (Bhatt et al. 2010). This recent increase in NDVI in the Arctic has been linked to greater plant biomass (Epstein et al. 2012, Raynolds et al. 2012), increased photosynthetic capacity, and an expansion of shrubs (Jia et al. 2002, Forbes et al. 2010). Substantial increases in biomass are predominately seen in subzones C–E (CAVM 2003, Walker et al. 2005), the three southernmost tundra subzones as identified in the Circumpolar Arctic Vegetation Map (CAVM)

(CAVM 2003, Walker et al. 2005), with an average increase in biomass of 19.8% from 1982–2010 (Epstein et al. 2012). The total increase in Alaskan tundra biomass during this time period was 7.8% (Epstein et al. 2012). Enhanced spectral resolution in remote sensing data could potentially help identify the nuances of these dynamics in plant biomass.

3.2 Vegetation Types throughout the North Slope of Alaska

The North Slope of Alaska extends from the Brooks Mountain Range to the Arctic Ocean (Murray 1978) and is largely dominated by either moist acidic tundra (MAT) or moist nonacidic tundra (MNT) (Muller et al. 1999). Soil acidity differentiates MAT from MNT communities, with MAT occurring on soils with pH < 5.0–5.5, and MNT occurring on soils with pH ≥ 5.0–5.5 (Walker et al. 1994, Walker et al. 2003a). MAT often occurs in areas with rolling topography and gravelly or silty soils overlain by an organic mat of up to 20 cm (Shaver and Chapin 1991). MAT is dominated by dwarf erect shrubs such as *Betula nana*, graminoid species such as *Eriophorum vaginatum*, and acidophilous mosses (e.g., *Aulacomium turgidum*) (Walker et al. 1994, Muller et al. 1999). MNT communities tend to occur along rivers and in the more northern Arctic Foothills and Coastal Plains (Jia et al. 2002). Mosses, graminoids (e.g., *Carex bigelowii*), and prostrate dwarf shrubs (e.g., *Dryas integrifolia*) dominate these communities (Jia et al. 2004) on calcium-rich, nonacidic (neutral pH) soils (Walker et al. 1998, Walker et al. 2001). *Betula nana* is absent from MNT communities due to its affinity for acidic soils (Muller et al. 1999). MNT differs in ecosystem structure and function from MAT, and generally has lower NDVI, LAI, and rates of photosynthesis and ecosystem respiration compared to MAT communities (Walker et al. 1995, Walker et al. 1998, Raynolds and Walker 2009).

Other vegetation types on the North Slope of Alaska include shrub tundra (ST) and mossy tussock tundra (MT). Shrub tundra is dominated by erect shrubs such as *Salix alaxensis*

and *Betula nana*, and is interspersed with graminoids, forbs, lichens, and mosses. Low shrub areas include shrubs approximately 40–60 cm in height, whereas heath shrub landscapes include shrubs approximately 10–20 cm in height (Bliss and Matveyeva 1992). On average, ST communities have lower albedo, lower summer soil temperatures, shallower summer active layer depths, and greater summer CO_2 exchange and sensible heat flux than other vegetation types (Sturm et al. 2005). Mossy tussock tundra is typified as an MAT community of tussock-forming sedges (e.g., *E. vaginatum*) with abundant *Sphagnum* mosses, and contributes greatly to biomass quantities in the Alaskan Arctic (Tenhunen et al. 1992).

3.3 Study Sites

The primary study site of Ivotuk, Alaska (68.49°N, 155.74°W) is located on the North Slope of the Brooks Mountain Range (Epstein et al. 2004b, Riedel et al. 2005a, Riedel et al. 2005b) and was one of seven sites established as part of the Arctic Transitions in the Land-Atmosphere System (ATLAS) project (McGuire 2003, Walker et al. 2003a, Walker et al. 2003b). Ivotuk is part of the Western Alaska Transect that starts in the north at Barrow and goes south through Atqasuk and Oumalik to Ivotuk (Jia et al. 2002, McGuire 2003, Walker et al. 2003a, Epstein et al. 2008). The Eastern Alaska Transect starts in the north at Prudhoe Bay and ends at Toolik Lake, a Long-Term Ecological Research (LTER) site (Walker et al. 1994, Chapin et al. 1995, Hobbie et al. 1999). Ivotuk is located in bioclimatic subzone E, the warmest and southernmost of the five tundra subzones (Figure 1.2) (Walker et al. 2003b). Ivotuk is largely a tussock tundra ecosystem also dominated by deciduous shrubs (Walker et al. 2003a) (Figure 1.3). It is located at an elevation of approximately 550 m (Epstein et al. 2004b), and is considered comparable to the Toolik Lake site (Riedel et al. 2005b). The site received an average annual rainfall of 202 mm, had a July maximum temperature of approximately 12 °C and an annual temperature of −10.9 °C

with a 110-day growing season from 1991–2001, a time period including the sampling period for the Ivotuk vegetation data (Jia et al. 2002, Riedel et al. 2005a, Riedel et al. 2005b). Aerial vegetation coverage is nearly 100% for Ivotuk, and all four plant communities in this study—MAT, MNT, MT, and ST—occur within a 2 km^2 area (Riedel et al. 2005a). ST had the greatest total aboveground peak growing season biomass (1291 g/m^2). MAT had a total aboveground biomass of 842 g/m^2 during peak growing season, while MT had a total of 804 g/m^2, and MNT had a total of 725 g/m^2 (Riedel et al. 2005a). Moss was the dominant contributor to biomass in MNT communities. Deciduous shrubs were the most dominant biomass component in ST communities, and graminoids were the most dominant contributor in MAT and MT communities (Table 1.1).

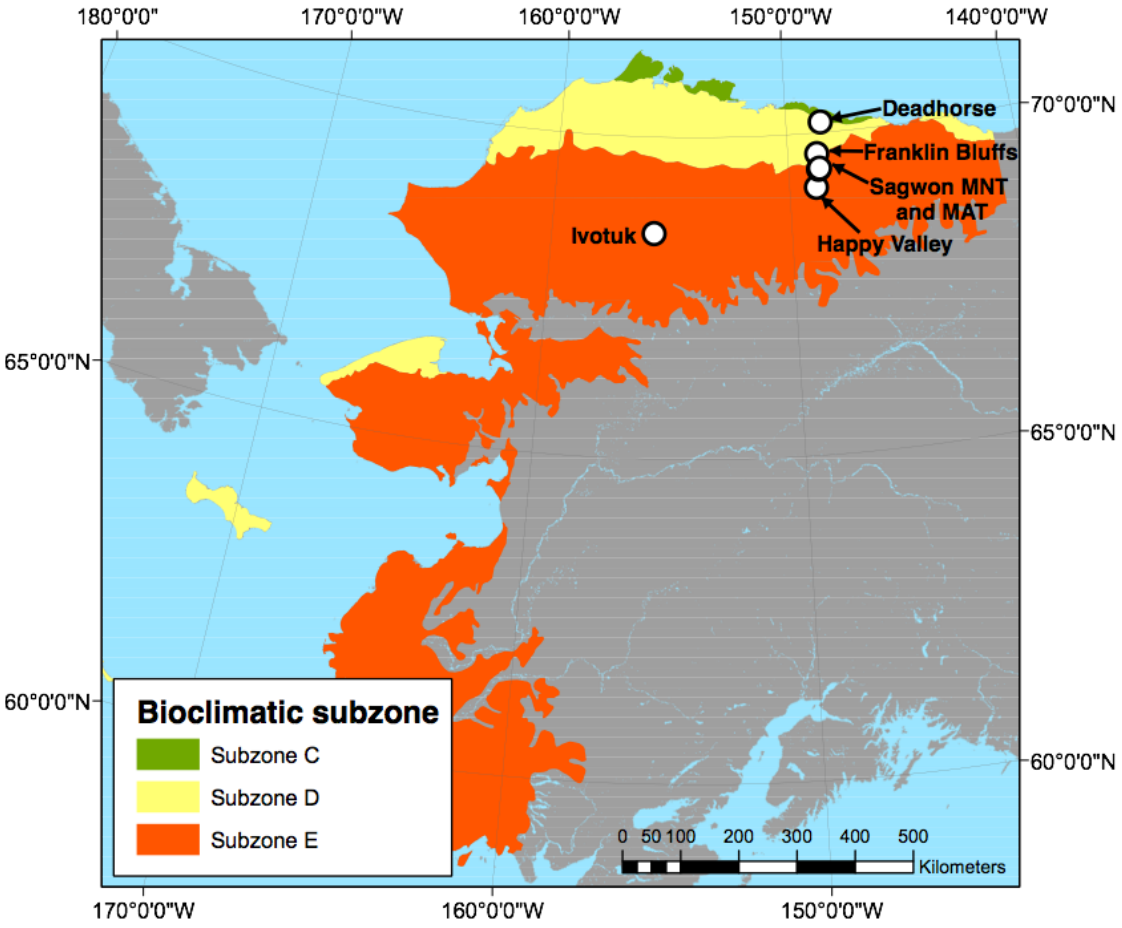

Figure 1.2. Location of Ivotuk, Deadhorse, Franklin Bluffs, Sagwon-MNT, Sagwon-MAT, and Happy Valley sites on the North Slope of Alaska within the Alaskan bioclimatic subzones of the Circumpolar Arctic Vegetation Map (CAVM 2003).

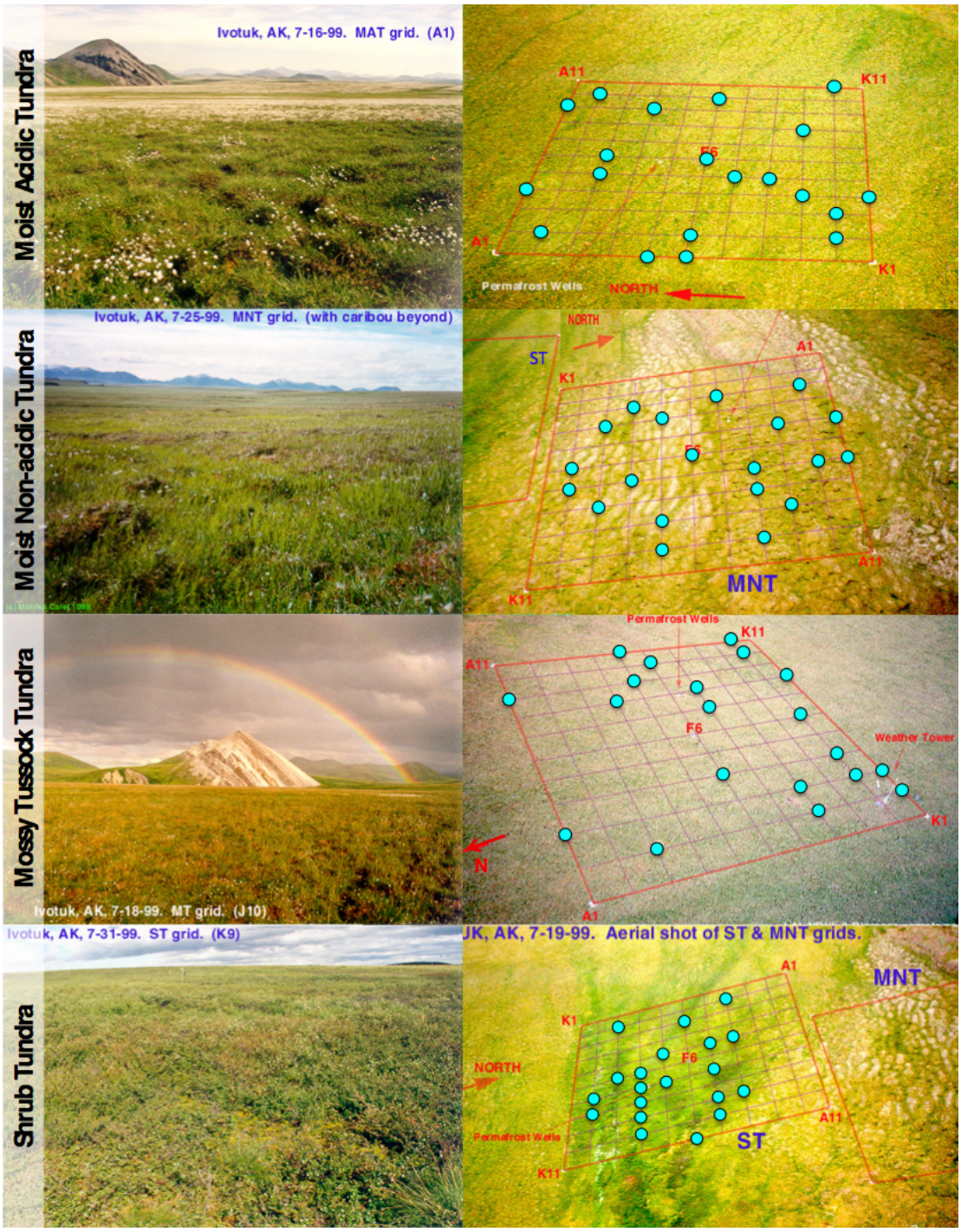

Figure 1.3. The four vegetation communities at Ivotuk, Alaska along with the grid and spectral sampling locations. Each point represents one sampling gridpoint. Study site images were taken between 16–31 July 1999. All grid images were taken on 19 July 1999 .

Table 1.1. Biomass percentages by plant functional type (PFT) and vegetation community type during early (7 June–7 July) and peak (16 July–17 August) growing season at Ivotuk, Alaska.

	Early (% biomass)				Peak (% biomass)			
	MAT	**MNT**	**MT**	**ST**	**MAT**	**MNT**	**MT**	**ST**
Deciduous shrub	15.6	3.7	3.6	64.1	18.8	5.1	3.6	55.9
Evergreen shrub	22.1	9.4	14.5	0.2	23.7	14.4	14.7	1.6
Forb	0.2	4.2	0.0	0.7	0.4	3.3	0.0	1.1
Graminoid	32.0	9.4	35.9	3.8	27.5	12.2	36.1	10.4
Lichen	4.9	3.0	3.1	1.3	5.7	3.6	3.3	2.4
Moss	25.2	70.3	42.4	29.9	23.9	61.5	42.4	28.6

Hyperspectral data from additional sites along the Dalton Highway (Buchhorn et al. 2013) on the North Slope of Alaska were used to evaluate the differentiation model developed at Ivotuk. The sites of Happy Valley (69.15°N, 148.85°W), Sagwon-MAT (69.43°N, 148.70°W), Sagwon-MNT (69.43°N, 148.7°W), Franklin Bluffs (69.67°N, 148.72°W), and Deadhorse (70.16°N, 148.46°W) are located along the Dalton Highway in Alaska and are part of the North American Arctic Transect (NAAT). Detailed descriptions of the sites can be found in (Kade et al. 2005, Raynolds et al. 2008b, Walker et al. 2008, Walker et al. 2011, Walker et al. 2012). Deadhorse, Franklin Bluffs, and Sagwon-MNT are MNT communities; Happy Valley and Sagwon-MAT are both MAT communities. Deadhorse is the northernmost site, occurs in the transition between subzones C and D, and was atypically wet during the 2012 data collection period (Buchhorn et al. 2013). Franklin Bluffs is in subzone D, and Sagwon MAT and MNT occur at the transition zone between subzones D and E. Happy Valley is the southernmost site, is located in subzone E, and most closely resembles the primary study site of Ivotuk.

3.4 Data Collection

One 100 m^2 vegetation grid was established in each community at Ivotuk for a total of four grids. Field spectroscopy data were collected during the 1999 growing season at biweekly intervals from 5 June–17 August. Spectroscopy data were grouped into early or peak growing season as determined by seasonal NDVI curves (Figure 1.1, Table 1.2). Data were grouped to avoid issues with low sample size for each of the individual sampling dates. Spectral measurements were taken using an Analytical Spectral Devices FieldSpec spectro-radiometer with a spectral resolution of 1.42 nm and a spectral range from 330–1062 nm. The sensor was held at nadir approximately 1.5 m above the vegetation surface, producing a 0.35 m^2 footprint with a 25° field of view (Riedel et al. 2005a). Spectral measurements were collected from ten random gridpoints established in each of the four vegetation grids. Spectra were taken from an additional ten gridpoints during peak growing season. Both the MNT and the ST grids exhibited some within-grid heterogeneity that was likely to influence the results. Within these grids, random sampling was stratified in such a way that sampling was representative of that particular vegetation community. Four replicate spectral measurements were taken at each gridpoint by moving 1 m in each cardinal direction from the actual gridpoint. Replicates were averaged to create the ten gridpoint spectral measurements per vegetation community per biweekly interval.

Data from the study sites of Deadhorse, Franklin Bluffs, Sagwon-MNT, Sagwon-MAT, and Happy Valley were collected during the 2012 growing season from 29 June to 11 July within the EyeSight-NAAT-Alaska expedition (Strauss and Buchhorn 2012, Buchhorn et al. 2013). Measurements were taken using two Spectra Vista Corporation GER1500 portable field spectro-radiometers with a spectral resolution of 1.5 nm and a spectral range from 330–1050 nm (Buchhorn et al. 2013). One 100 m^2 vegetation grid was sampled from each of the study sites.

The grid was divided into 1 × 1 m quadrats for a total of 100 observations. These values were then averaged to produce mean reflectances per site.

Table 1.2. Sampling dates and total number of observations per vegetation community during the early (7 June–7 July) and peak (16 July–17 August) 1999 growing season at Ivotuk, Alaska.

Growing Season	MAT	MNT	MT	ST
Early	7 June, 26 June, 2 July (n = 42)	10 June, 25 June, 2 July (n = 45)	10 June, 25 June, 2 July (n = 41)	10 June, 26 June, 7 July (n = 37)
Peak	16 July, 27 July, 17 August (n = 40)	16 July, 27 July, 17 August (n = 43)	16 July, 27 July (n = 33)	16 July, 27 July, 7 August (n = 33)

3.5 Spectral Processing

All spectra were evaluated visibly for potentially bad data. Outliers were removed from the dataset in an effort to achieve a more diagnostic spectral signature; this resulted in an underrepresentation of MT and ST during peak growing season. Spectroscopy data were resampled to 5 nm wide hyperspectral narrowbands ranging from 400–1000 nm. Resampling increases the signal-to-noise ratio, reduces redundancy issues among predictor variables, and makes the results potentially more transferable from Ivotuk to the five other Alaskan sites, for which data were collected with a different spectro-radiometer.

In addition to the original reflectances, data were also analyzed using continuum removal. Continuum removal normalizes spectra by establishing a baseline from which to compare absorption features (Clark and Roush 1984), and this methodology can be used to effectively discriminate among vegetation types (Buchhorn et al. 2013). Continuum removal for three absorption feature regions (blue, red, and water) was performed using ENVI (Exelis Visual

Information Solutions, Boulder, CO, USA). Averaged reflectances per vegetation community were used for continuum-removal analysis of the three absorption features: (1) blue absorption (400–550 nm); (2) red absorption (560–750 nm); and (3) water absorption (930–1055 nm). Spectral metrics such as maximum band depth, HNB at maximum band depth, width of the absorption feature at half maximum absorption depth, and area of the absorption feature were analyzed for these three features (Kokaly and Skidmore 2015).

3.6 Data Analysis

To decrease the amount of redundant hyperspectral narrow bands (HNBs), overcome the Hughes's phenomenon (Hughes 1968, Marshall and Thenkabail 2014), and identify optimal HNBs for distinguishing among arctic vegetation communities, I used a two-step sparse partial least squares (SPLS) and linear discriminant analysis (LDA). SPLS regression was done using the SIMPLS algorithm from the "spls" package in R (Chung et al. 2013). SPLS is a variable selection and dimension reduction technique that is useful for spectroscopic analysis, as it is unaffected by issues such as high collinearity among predictor variables and cases where $p > n$. The resulting latent vectors are in terms of the original HNBs as a result of the sparsity parameter in SPLS (Chun and Keles 2010).

The HNBs with the greatest loading coefficients from the SPLS (top 10%) were then put through an LDA to discriminate among the four vegetation communities at Ivotuk. A simple random sample of approximately one-half of the Ivotuk data were used as a training set for the model, and then the model was applied to the remaining test set of Ivotuk data. Following this, peak growing season data from Ivotuk were used as the training set and tested against the five study sites of Deadhorse, Franklin Bluffs, Sagwon-MNT, Sagwon-MAT, and Happy Valley.

4. Results

4.1 Sparse Partial Least Squares (SPLS) and Linear Discriminant Analysis (LDA)

SPLS identified eight optimal HNBs during early growing season and twelve optimal HNBs during peak growing season (Table 1.3). The majority of HNBs for early and peak growing season were in the NIR wavelength region (Figure 1.4), and the spectral locations of the most significant HNBs differ seasonally. HNBs in the blue, green, and NIR load highest during the early growing season, whereas HNBs in the NIR load highest during the peak growing season. Overall classification accuracy of the LDA was greater during peak growing season at 94% compared to early growing season at 84% (Table 1.4; Figure 1.5). MT was the best classified community during early growing season at 100%. ST had the lowest classification accuracy during early growing season at 65%. MNT, MT, and ST were all classified at 100% during peak growing season. MAT was classified at 80% during peak growing season.

Table 1.3. Top ten percent of significant hyperspectral narrowbands (HNBs) for all four vegetation communities and overall classification accuracy of the linear discriminant analysis (LDA) using the optimal HNBs. All Wilks's lambda values are significant ($p < 0.001$).

Sampling Period	Significant HNBs (nm)	Wilks' Lambda	Sum of Eigenvalues	Overall Classification Accuracy Using the Optimal HNBs Only (%)
Early	405, 505, 690, 770, 840, 905, 920, 980	0.03	8.41	84
Peak	405, 450, 790, 795, 800, 845, 850, 910, 940, 975, 980, 990	0.01	12.39	94

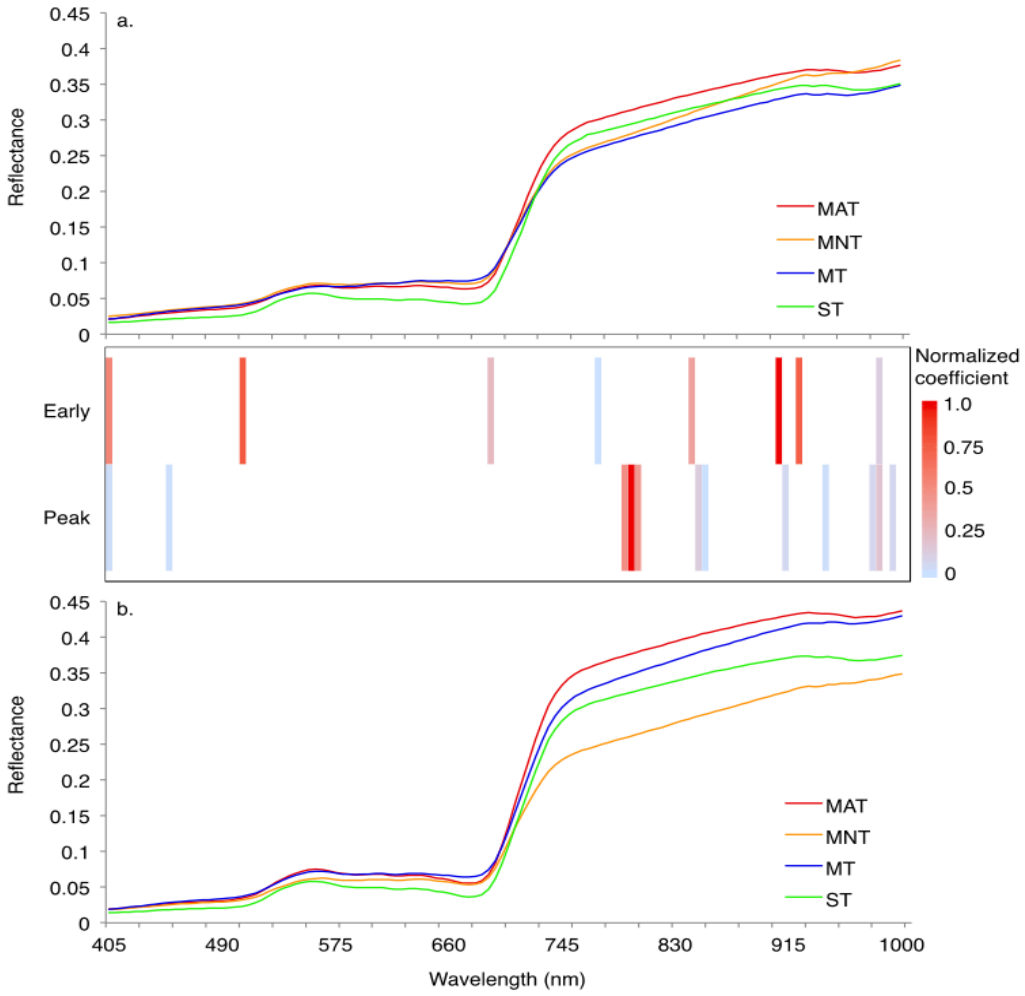

Figure 1.4. Mean reflectance spectra for the four vegetation communities during early (a) and peak (b) growing season at Ivotuk, Alaska in 1999. Reflectance spectra are shown along with the top ten percent of optimal hyperspectral narrowbands (HNBs) and their normalized coefficients for the first discriminant function.

Table 1.4. Confusion matrices and classification accuracies at Ivotuk, Alaska using the top ten percent of significant hyperspectral narrowbands (HNBs).

Classification Accuracy (%)		**Early Growing Season**				**Classification Accuracy (%)**		**Peak Growing Season**			
		MAT	MNT	MT	ST			MAT	MNT	MT	ST
73	MAT	16	-	4	2	80	MAT	16	-	-	4
92	MNT	1	2	1	-	100	MNT	-	23	-	-
100	MT	-	-	21	-	100	MT	-	-	13	-
65	ST	2	-	4	11	100	ST	-	-	-	13

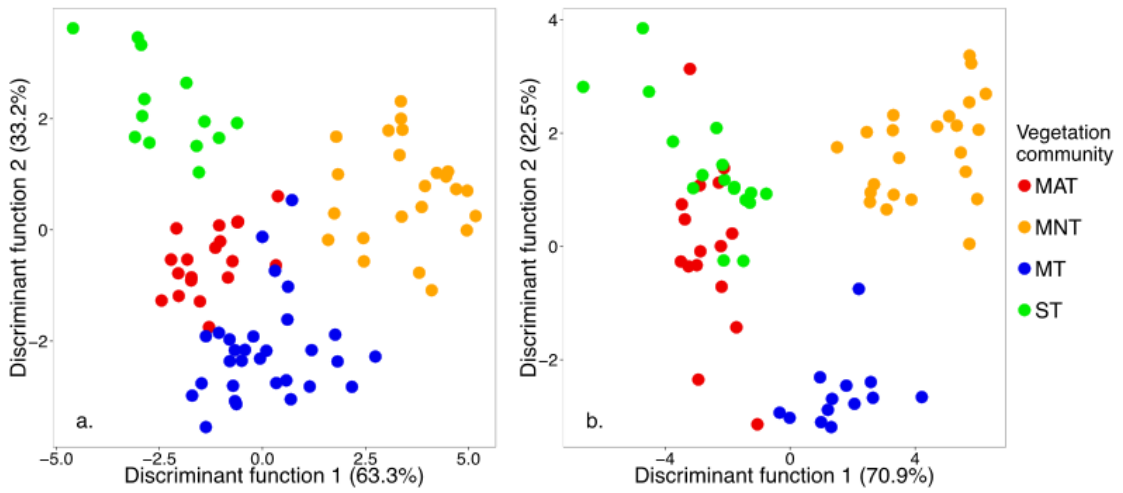

Figure 1.5. First two functions derived from linear discriminant analysis for the four vegetation communities at Ivotuk, Alaska using the top ten percent of optimal hyperspectral narrowbands (HNBs) during early (a) and peak (b) growing season.

4.2 Continuum Removal

Continuum-removed reflectance spectra were examined in the blue, red, and water absorption features. Continuum-removed reflectance spectra did not always exhibit clear distinctions among the four vegetation communities during early (Figure 1.6) or peak growing season (Figure 1.7). Maximum absorption depth for the blue absorption feature was found at 495–500 nm for all vegetation communities during early and peak growing season (Table 1.5). Maximum absorption depth occurred at 680 nm for the red absorption feature, and 965–980 nm for the water absorption feature. ST had the greatest values for the three spectral metrics of maximum band depth, full width at half maximum band depth, and area of absorption feature. Scaled continuum-removed reflectances indicate that differences among vegetation community types are most pronounced in the 400–500 nm region of the blue absorption feature. Differences

are most pronounced in the 560–680 nm range in the red absorption feature, and between 930–945 nm for the water absorption feature.

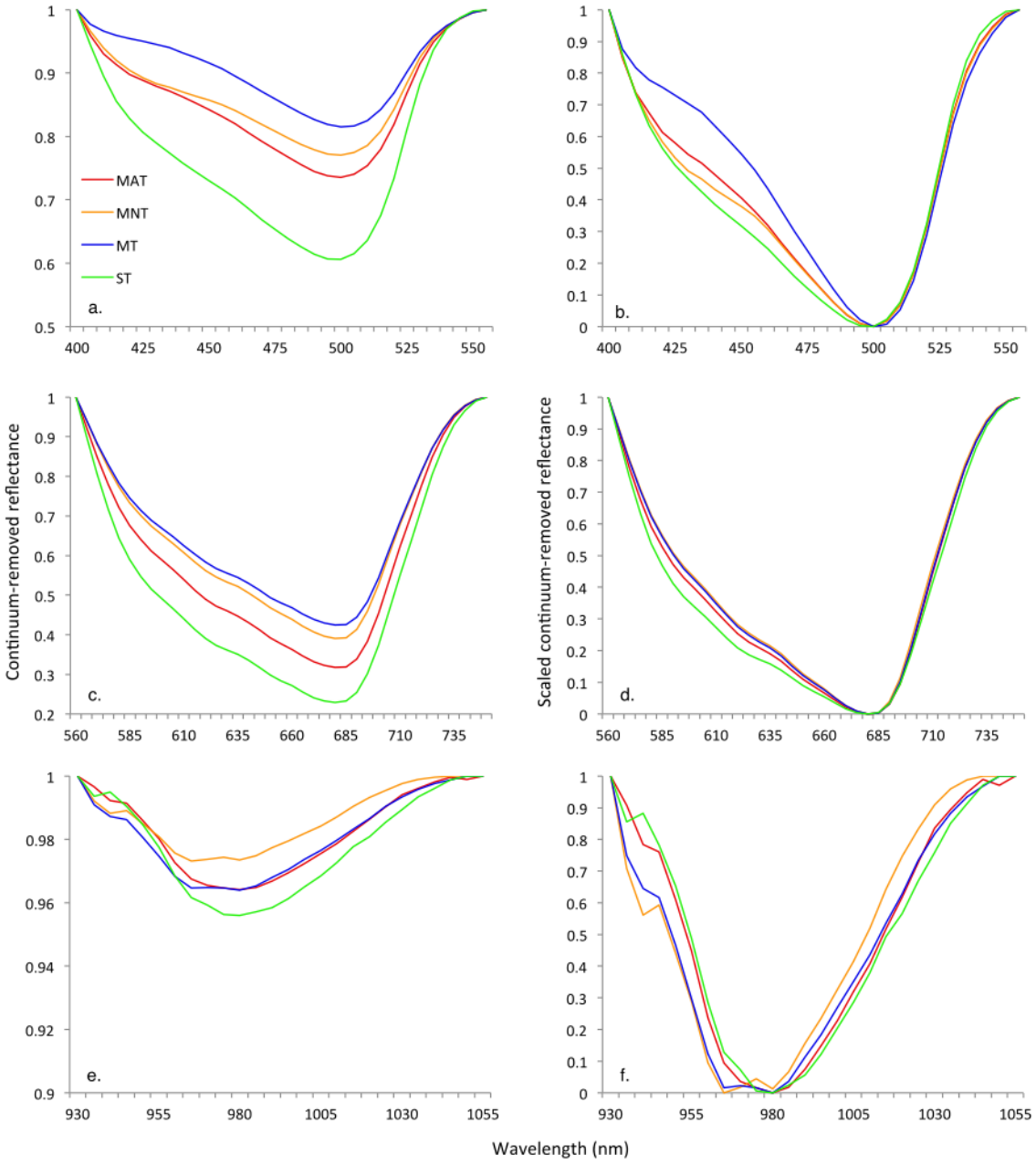

Figure 1.6. Average continuum-removed and scaled continuum-removed reflectance spectra at Ivotuk, Alaska for the blue (a,b), red (c,d), and water (e,f) absorption features during early growing season.

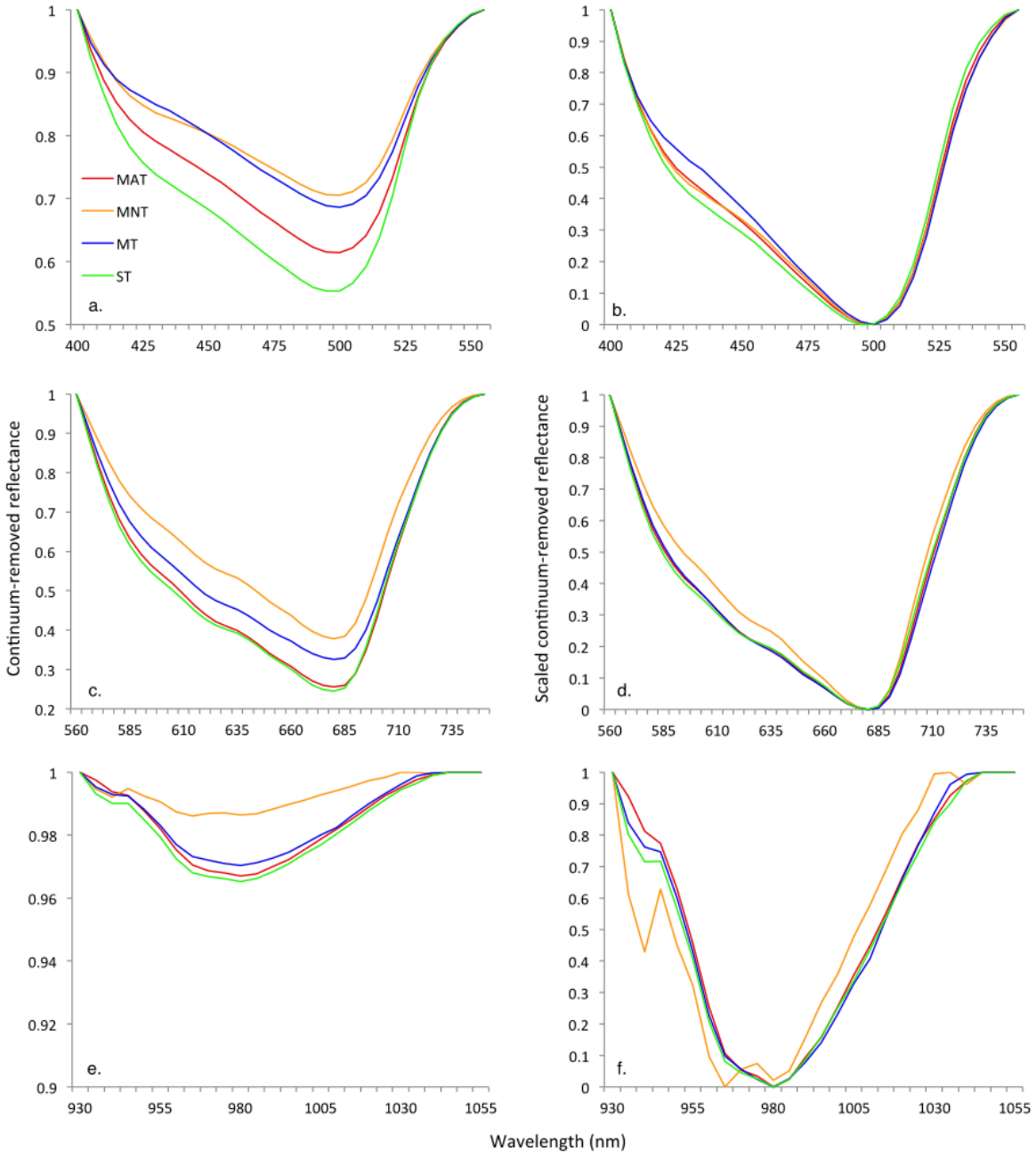

Figure 1.7. Average continuum-removed and scaled continuum-removed reflectance spectra at Ivotuk, Alaska for the blue (a,b), red (c,d), and water (e,f) absorption features during peak growing season.

Table 1.5. Spectral metrics from continuum-removal analysis for the blue, red, and water absorption features at Ivotuk.

		Blue				Red				Water			
Growing Season	**Vegetation Community**	**HNB of Maximum Depth (nm)**	**Maximum Band Depth**	**Full Width at Half Maximum Band Depth (nm)**	**Area of Absorption Feature**	**HNB of Maximum Depth (nm)**	**Maximum Band Depth**	**Full Width at Half Maximum Band Depth (nm)**	**Area of Absorption Feature**	**HNB of Maximum Depth (nm)**	**Maximum Band Depth**	**Full Width at Half Maximum Band Depth**	**Area of Absorption Feature**
Early	MAT	500	0.26	87.53	22.8	680	0.68	125.01	78.1	980	0.04	61.66	2.2
	MNT	500	0.23	96.52	20.2	680	0.61	120.23	67.6	965	0.03	65.44	1.7
	MT	500	0.18	71.53	14.4	680	0.58	121.64	64.6	980	0.04	67.04	2.4
	ST	500	0.39	98.56	35.6	680	0.77	131.28	92.2	980	0.04	60.69	2.8
Peak	MAT	500	0.39	101.14	35.5	680	0.74	125.02	84.6	980	0.03	58.99	2.0
	MNT	500	0.29	102.65	27.2	680	0.62	113.72	65.7	965	0.01	59.64	0.8
	MT	500	0.31	92.98	28.2	680	0.67	125.20	77.2	980	0.03	62.96	1.8
	ST	495	0.45	103.67	41.6	680	0.76	125.79	86.0	980	0.03	40.70	2.2

4.3 Predicting Vegetation Community Types at the Five Dalton Highway Test Sites

Peak growing season spectra from Ivotuk were used as a training set to create models that were then used to predict plant community types at the five other Alaska sites. Only MAT and MNT vegetation communities were used for this analysis as MT and ST communities were not sampled at the other sites. This subset of the Ivotuk data was put through the two-step SPLS and LDA to determine optimal HNBs. The resulting model was then applied to the five sites of Deadhorse, Franklin Bluffs, Sagwon-MNT, Sagwon-MAT, and Happy Valley.

This analysis identified nine optimal HNBs. Bands in the red edge were the most common and the most significant to the model (Table 1.6, Figure 1.8). Classification accuracy was better for MAT communities than MNT communities, and generally better at sites more similar to, and geographically nearer to, Ivotuk. Sagwon-MAT was the best classified community (91%), followed by Happy Valley (90%). The closest MNT community to Ivotuk is Sagwon MNT, which had the greatest classification accuracy of the three MNT communities (70%). Both Deadhorse and Franklin Bluffs are more northern than the rest of the sites, and had similar classification accuracies of 56% and 55%, respectively.

Table 1.6. Optimal hyperspectral narrowbands (HNBs) for the five Dalton Highway sites and overall classification accuracy of the linear discriminant analysis (LDA) using the top ten percent of optimal HNBs.

Optimal HNBs (nm)	Site and Community Classification	Overall Classification Accuracy Using the Optimal HNBs Only (%)
470, 685, 690, 695, 710, 715, 760, 935, 980	Deadhorse	56
	Franklin Bluffs	55
	Sagwon-MNT	70
	Sagwon-MAT	91
	Happy Valley	90

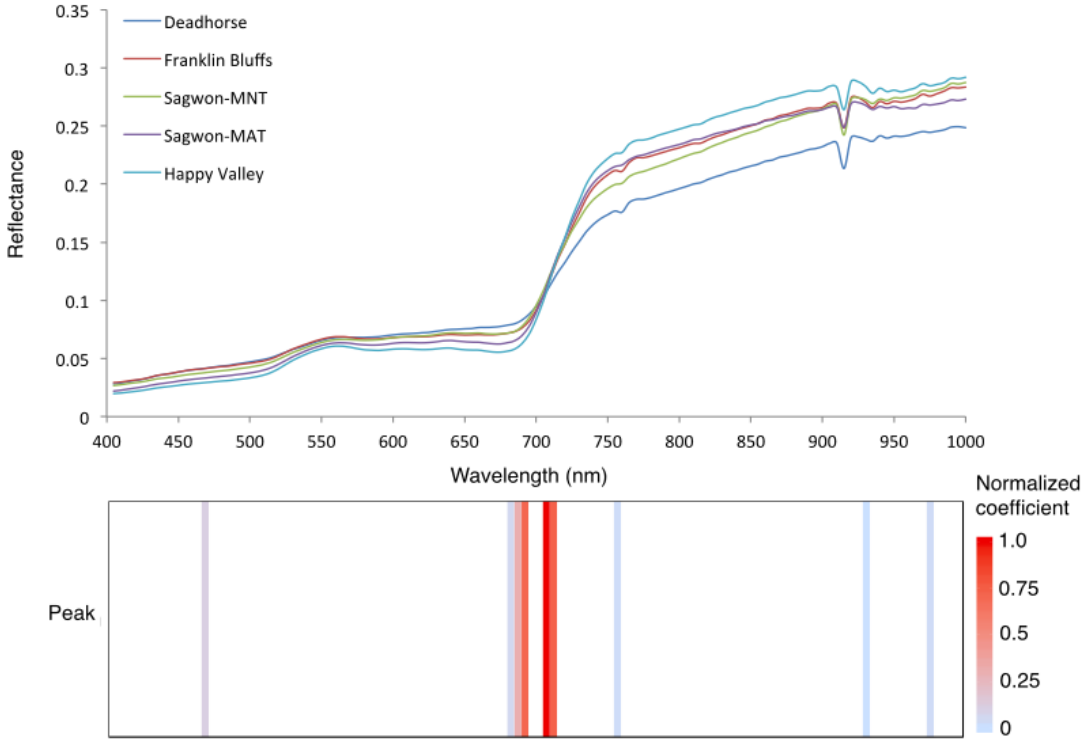

Figure 1.8. Mean reflectance spectra for the five Dalton Highway test sites. Reflectance spectra are shown along with the top ten percent of optimal hyperspectral narrowbands (HNBs) and their normalized coefficients for the first discriminant function.

5. Discussion

This study uses HNBs and a two-step SPLS and LDA approach to differentiate among vegetation communities at Ivotuk, Alaska. This differentiation model was then applied to the sites of Deadhorse, Franklin Bluffs, Sagwon-MNT, Sagwon-MAT, and Happy Valley. Continuum-removal findings from Ivotuk are similar to other vegetation studies along the North Slope of Alaska that have identified maxima in the blue and red absorption features. Past research on MAT and MNT vegetation communities has identified absorption maxima of 500 nm and 680 nm for the Dalton Highway data used in this study (Buchhorn et al. 2013). Findings at Ivotuk are similar to these, with a chlorophyll and carotenoid absorption maximum occurring between 495 and 500 nm, and a second chlorophyll maximum at 680 nm (Figures 1.6 and 1.7). The greatest changes in maximum band depth from early to peak growing season were found in the blue absorption feature, indicating greater absorption by chlorophyll and carotenoids during peak growing season.

HNBs located in areas associated with pigments (400–700 nm) had greater linear discriminant coefficients and were more frequently found to be significant during the early growing season. HNBs associated with structural tissue (NIR) were more significant during peak growing season, indicating an increased reliance on vegetation structure and morphological differences among species to differentiate tundra communities during peak growing season. Separability at Ivotuk relied heavily on HNBs outside the typical range of broad-band NDVI. Although HNBs in the NIR were significant, they were never used in a model that also included the red wavelengths. Furthermore, the most significant bands for the Dalton Highway test sites were located in the red edge (680–725 nm), which is typically outside the range of broad-band NDVI. Whereas the vegetation community reflectance at Ivotuk would appear homogeneous

with regard to NDVI outside of the peak growing season (Riedel et al. 2005a), this study shows that hyperspectral remote sensing data can be used to discriminate among these vegetation communities during the early growing season. The communities of MAT and ST at Ivotuk were the most compositionally similar with regard to the ratio of vascular to non-vascular vegetation, and were the most commonly misclassified during early and peak growing season at Ivotuk. MAT and ST are comprised of approximately 70% vascular plant and 30% non-vascular. MNT has the inverse composition, and MT composition is almost equal between vascular and non-vascular vegetation, and was the only vegetation community never misclassified at Ivotuk. During peak growing season, MAT was exclusively misclassified as ST, highlighting the importance of vegetation structure for tundra community discrimination during peak growing season.

Among the four vegetation types at Ivotuk, ST had the lowest reflectances in the visible spectrum during both early and peak growing season, and MAT had the greatest absolute reflectances for both early and peak growing season. Differences among vegetation communities in the NIR wavelength region occurred during the early growing season, yet were amplified during peak growing season. Other research in the Alaskan Arctic has identified five bands useful for discriminating among vascular and non-vascular vegetation located in the blue, red, and NIR regions (Huemmrich et al. 2013). This study suggests that similar regions of the spectrum can be used to discriminate among vegetation communities also using hyperspectral remote sensing data.

The MAT vegetation types at Ivotuk are most similar to the southernmost test site of Happy Valley. Reflectances in the NIR were greater at Ivotuk than Happy Valley and the other four Dalton Highway test sites. Happy Valley had the lowest reflectances in the visible regions

and the highest reflectances in the NIR wavelength regions of the Dalton Highway sites. Sagwon-MNT is the most similar MNT site to the MNT grid at Ivotuk, and like the MNT spectral signature at Ivotuk, had lower reflectances in the NIR than other sites with the exception of Deadhorse, which was unusually wet during the data collection period. Sagwon-MNT had lower reflectances in the NIR than the MNT community at Ivotuk, and greater reflectance in the red trough. Franklin Bluffs and Sagwon MAT exhibited similar reflectances in the NIR, but differed in the visible wavelength region, where reflectance for Sagwon MAT more closely mirrored Happy Valley, the only other Dalton Highway MAT community.

6. Conclusions

This study presents an example of the potential for hyperspectral remote sensing to improve upon the classification of tundra vegetation communities in the Arctic. Field research in the Arctic is difficult and expensive. Ground-based remote sensing studies are critical, as they allow for the development of spectral relationships that can then potentially be extrapolated to satellite remote sensing. The discriminability of MAT, MNT, MT, and ST communities is improved upon through the use of hyperspectral remote sensing in this study. Hyperspectral remote sensing allows for the inclusion of both a wider range of spectral data and finer resolution spectral data than traditional multi-spectral approaches. Establishing these relationships allows for the identification of HNBs on hyperspectral satellites that may be valuable for distinguishing among vegetation communities. Such forthcoming projects include the NASA Hyperspectral Infrared Imager (HyspIRI) and the German Environmental Mapping and Analysis Program (EnMAP). Establishing the spectral differences among these vegetation communities using field spectroscopy data facilitates the potential for monitoring of changes occurring in vegetation communities as a result of increasing temperatures in the Arctic.

7. References

ATLAS project website.

Bhatt, U. S., D. A. Walker, M. K. Raynolds, J. C. Comiso, H. E. Epstein, G. Jia, R. Gens, J. E. Pinzon, C. J. Tucker, C. E. Tweedie, and P. J. Webber. 2010. Circumpolar Arctic Tundra Vegetation Change Is Linked to Sea Ice Decline. Earth Interactions **14**:1-20.

Bliss, L. C., and N. V. Matveyeva. 1992. Circumpolar Arctic Vegetation.*in* F. S. Chapin III, R. L. Jefferies, A. Reynolds, G. R. Shaver, and J. Svoboda, editors. Arctic Ecosystems in a Changing Climate. Academic Press, Inc. , San Diego.

Boelman, N. T., L. Gough, J. R. McLaren, and H. Greaves. 2011. Does NDVI reflect variation in the structural attributes associated with increasing shrub dominance in arctic tundra? Environmental Research Letters **6**:035501.

Buchhorn, M., D. Walker, B. Heim, M. Raynolds, H. Epstein, and M. Schwieder. 2013. Ground-Based Hyperspectral Characterization of Alaska Tundra Vegetation along Environmental Gradients. Remote Sensing **5**:3971-4005.

CAVM. 2003. Circumpolar Arctic Vegetation Map. (1:7,500,000 scale), Conservation of Arctic Flora and Fauna (CAFF) Map No. 1. U.S. Fish and Wildlife Service, Anchorage, Alaska.

Chapin, F. S., G. R. Shaver, A. E. Giblin, K. J. Nadelhoffer, and J. A. Laundre. 1995. Responses of Arctic Tundra to Experimental and Observed Changes in Climate. Ecology **76**:694-711.

Chun, H., and S. Keles. 2010. Sparse partial least squares regression for simultaneous dimension reduction and variable selection. Journal of the Royal Statistical Society. Series B (Methodological) **72**:3-25.

Chung, D., H. Chun, and S. Keles. 2013. spls: Sparse Partial Least Squares (SPLS) Regression and Classification. R Package Vignette.

Clark, R. N., and T. L. Roush. 1984. Reflectance spectroscopy: Quantitative analysis techniques for remote sensing applications. Journal of Geophysical Research **89**:6329.

Comiso, J. C., and D. K. Hall. 2014. Climate trends in the Arctic as observed from space. Wiley Interdisciplinary Reviews: Climate Change **5**:389-409.

Curran, P. J. 1989. Remote Sensing of Foliar Chemistry. Remote Sensing of Environment **30**:271-278.

DeMarco, J., M. C. Mack, and M. S. Bret-Harte. 2014. Effects of arctic shrub expansion on biophysical versus biogeochemical drivers of litter decomposition. Ecology.

Elmendorf, S. C., G. H. Henry, R. D. Hollister, R. G. Bjork, A. D. Bjorkman, T. V. Callaghan, L. S. Collier, E. J. Cooper, J. H. Cornelissen, T. A. Day, A. M. Fosaa, W. A. Gould, J. Gretarsdottir, J. Harte, L. Hermanutz, D. S. Hik, A. Hofgaard, F. Jarrad, I. S. Jonsdottir, F. Keuper, K. Klanderud, J. A. Klein, S. Koh, G. Kudo, S. I. Lang, V. Loewen, J. L. May, J. Mercado, A. Michelsen, U. Molau, I. H. Myers-Smith, S. F. Oberbauer, S. Pieper, E. Post, C. Rixen, C. H. Robinson, N. M. Schmidt, G. R. Shaver, A. Stenstrom, A. Tolvanen, O. Totland, T. Troxler, C. H. Wahren, P. J. Webber, J. M. Welker, and P. A. Wookey. 2012. Global assessment of experimental climate warming on tundra vegetation: heterogeneity over space and time. Ecol Lett **15**:164-175.

Epstein, H. E., M. P. Calef, M. D. Walker, F. S. Chapin III, and A. M. Starfield. 2004. Detecting changes in arctic tundra plant communities in response to warming over decadal time scales. Global Change Biology **10**:1325-1334.

Epstein, H. E., M. K. Raynolds, D. A. Walker, U. S. Bhatt, C. J. Tucker, and J. E. Pinzon. 2012. Dynamics of aboveground phytomass of the circumpolar Arctic tundra during the past three decades. Environmental Research Letters **7**:015506.

Epstein, H. E., D. A. Walker, M. K. Raynolds, G. J. Jia, and A. M. Kelley. 2008. Phytomass patterns across a temperature gradient of the North American arctic tundra. Journal of Geophysical Research **113**.

Forbes, B. C., M. M. Fauria, and P. Zetterberg. 2010. Russian Arctic warming and 'greening' are closely tracked by tundra shrub willows. Global Change Biology **16**:1542-1554.

Hansen, J., R. Ruedy, M. Sato, and K. Lo. 2010. Global Surface Temperature Change. Reviews of Geophysics **48**.

Hinzman, L. D., C. J. Deal, A. D. McGuire, S. H. Mernild, I. V. Polyakov, and J. E. Walsh. 2013. Trajectory of the Arctic as an integrated system. Ecological Applications **23**:1837-1868.

Hobbie, S. E., A. Shevtsova, and F. S. Chapin III. 1999. Plant Responses to Species Removal and Experimental Warming in Alaskan Tussock Tundra. Oikos **84**:417-434.

Hope, A., J. S. Kimball, and D. Stow. 1993. The relationship between tussock tundra spectral reflectance properties and biomass and vegetation composition. International Journal of Remote Sensing **14**:1861-1874.

Huemmrich, F., J. A. Gamon, C. E. Tweedie, P. Campbell, D. R. Landis, and E. Middleton. 2013. Arctic Tundra Vegetation Functional Types Based on Photosynthetic Physiology and Optical Properties. IEEE Journal of Selected Topics in Applied Earth Observations and Remote Sensing **6**:265-275.

Huemmrich, K. F., J. A. Gamon, C. E. Tweedie, S. F. Oberbauer, G. Kinoshita, S. Houston, A. Kuchy, R. D. Hollister, H. Kwon, and M. Mano. 2010a. Remote sensing of tundra gross ecosystem productivity and light use efficiency under varying temperature and moisture conditions. Remote Sensing of Environment **114**:481-489.

Huemmrich, K. F., G. Kinoshita, J. A. Gamon, S. Houston, H. Kwon, and W. C. Oechel. 2010b. Tundra carbon balance under varying temperature and moisture regimes. Journal of Geophysical Research **115**.

Hughes, M. 1968. On the mean accuracy of statistical pattern recognizers. IEEE Transactions on Information Theory **14**:55-63.

Jia, G. J., H. E. Epstein, and D. Walker. 2002. Spatial characteristics of AVHRR-NDVI along latitudinal transectsin northern Alaska. Journal of Vegetation Science **13**:315-326.

Jia, G. J., H. E. Epstein, and D. A. Walker. 2004. Controls over intra-seasonal dynamics of AVHRR NDVI for the Arctic tundra in northern Alaska. International Journal of Remote Sensing **25**:1547-1564.

Kade, A., D. A. Walker, and M. K. Raynolds. 2005. Plant communities and soils in cryoturbated tundra along a bioclimate gradient in the Low Arctic, Alaska. Phytocoenologia **35**:761-820.

Kaufman, D. S., D. P. Schneider, N. P. McKay, C. M. Ammann, R. S. Bradley, K. R. Briffa, G. H. Miller, B. L. Otto-Bliesner, J. T. Overpeck, B. M. Vinther, and M. Arctic Lakes 2k Project. 2009. Recent warming reverses long-term arctic cooling. Science **325**:1236-1239.

Kokaly, R. F., and A. K. Skidmore. 2015. Plant phenolics and absorption features in vegetation reflectance spectra near 1.66 μm. International Journal of Applied Earth Observation and Geoinformation.

Laidler, G. J., P. Treitz, and D. Atkinson. 2008. Remote sensing of Arctic vegetation: Relations between the NDVI, spatial resolution and vegetation cover on Boothia Peninsula, Nunavut. Arctic **61**:1-13.

Marshall, G. J., and P. Thenkabail. 2014. Biomass Modeling of Four Leading World Crops Using Hyperspectral Narrowbands in Support of HyspIRI Mission. Photogrammetric Engineering & Remote Sensing **80**:757-772.

McGuire, A. D. 2003. Arctic Transitions in the Land–Atmosphere System (ATLAS): Background, objectives, results, and future directions. Journal of Geophysical Research **108**.

Muller, S. V., A. E. Racoviteanu, and D. A. Walker. 1999. Landsat MSS-derived land-cover map of northern Alaska: extrapolation methods and a comparison with photo-interpreted and AVHRR-derived maps. International Journal of Remote Sensing **20**:2921-2946.

Murray, D. F. 1978. Vegetation, Floristics, and Phytogeography of Northern Alaska. Pages 19-36 *in* L. L. Tieszen, editor. Vegetation and Production Ecology of an Alaskan Arctic Tundra. Springer-Verlag, New York.

Myers-Smith, I. H., B. C. Forbes, M. Wilmking, M. Hallinger, T. Lantz, D. Blok, K. D. Tape, M. Macias-Fauria, U. Sass-Klaassen, E. Lévesque, S. Boudreau, P. Ropars, L. Hermanutz, A. Trant, L. S. Collier, S. Weijers, J. Rozema, S. A. Rayback, N. M. Schmidt, G. Schaepman-Strub, S. Wipf, C. Rixen, C. B. Ménard, S. Venn, S. Goetz, L. Andreu-Hayles, S. Elmendorf, V. Ravolainen, J. Welker, P. Grogan, H. E. Epstein, and D. S. Hik. 2011. Shrub expansion in tundra ecosystems: dynamics, impacts and research priorities. Environmental Research Letters **6**:045509.

Olthof, I., and R. Latifovic. 2007. Short-term response of arctic vegetation NDVI to temperature anomalies. International Journal of Remote Sensing **28**:4823-4840.

Raynolds, M., and D. Walker. 2009. Effects of deglaciation on circumpolar distribution of arctic vegetation. Canadian Journal of Remote Sensing **35**:118-129.

Raynolds, M. K., D. A. Walker, H. E. Epstein, J. E. Pinzon, and C. J. Tucker. 2012. A new estimate of tundra-biome phytomass from trans-Arctic field data and AVHRR NDVI. Remote Sensing Letters **3**:403-411.

Raynolds, M. K., D. A. Walker, C. A. Munger, C. M. Vonlanthen, and A. N. Kade. 2008. A map analysis of patterned-ground along a North American Arctic Transect. Journal of Geophysical Research **113**.

Riedel, S., H. E. Epstein, D. A. Walker, D. L. Richardson, M. P. Calef, E. Edwards, and A. Moody. 2005a. Spatial and Temporal Heterogeneity of Vegetation Properties among Four Tundra Plant Communities at Ivotuk, Alaska, U. S. A. Arctic, Antarctic, and Alpine Research **37**:25-33.

Riedel, S. M., H. E. Epstein, and D. A. Walker. 2005b. Biotic controls over spectral reflectance of arctic tundra vegetation. International Journal of Remote Sensing **26**:2391-2405.

Serreze, M. C., and J. A. Francis. 2006. The Arctic Amplification Debate. Climatic Change **76**:241-264.

Shaver, G. R., and F. S. Chapin. 1991. Production: Relationships and Element Cycling in Contrasting Arctic Vegetation Types. Ecological Monographs **61**:1-31.

Silapaswan, C., D. Verbyla, and A. D. McGuire. 2001. Land Cover Change on the Seward Peninsula: The Use of Remote Sensing to Evaluate the Potential Influences of Climate Warming on Historical Vegetation Dynamics. Canadian Journal of Remote Sensing **27**:542-554.

Stow, D. A., A. Hope, D. McGuire, D. Verbyla, J. Gamon, F. Huemmrich, S. Houston, C. Racine, M. Sturm, K. Tape, L. Hinzman, K. Yoshikawa, C. Tweedie, B. Noyle, C. Silapaswan, D. Douglas, B. Griffith, G. Jia, H. Epstein, D. Walker, S. Daeschner, A. Petersen, L. Zhou, and R. Myneni. 2004. Remote sensing of vegetation and land-cover change in Arctic Tundra Ecosystems. Remote Sensing of Environment **89**:281-308.

Strauss, J., and M. Buchhorn. 2012. Expeditions to the permafrost 2012: Alaskan North Slope/Itkilik, Thermokarst in Central Yakutia, EyeSight-NAAT-Alaska. Alfred-Wegener-Institut für Polar-und Meeresforschung, Bremerhaven, Germany.

Sturm, M., J. P. McFadden, G. E. Liston, F. S. Chapin III, C. Racine, and J. Holmgren. 2001a. Snow-Shrub Interactions in Arctic Tundra: A Hypothesis with Climate Implications. Journal of Climate **14**:336-344.

Sturm, M., C. Racine, and K. D. Tape. 2001b. Increasing shrub abundance in the Arctic. Nature **411**:1251-1256.

Sturm, M., J. P. Schimel, G. J. Michaelson, J. M. Welker, S. F. Oberbauer, G. E. Liston, J. Fahnestock, and V. E. Romanovsky. 2005. Winter Biological Processes Could Help Convert Arctic Tundra to Shrubland. BioScience **55**:17-26.

Tape, K. E. N., M. Sturm, and C. Racine. 2006. The evidence for shrub expansion in Northern Alaska and the Pan-Arctic. Global Change Biology **12**:686-702.

Tenhunen, J. D., O. L. Lange, S. Hahn, R. Siegwolf, and S. F. Oberbauer. 1992. The Ecosystem Role of Poikilohydric Tundra Plants. Pages 213-239 *in* F. S. Chapin III, R. L. Jefferies, J. F. Reynolds, and G. R. Shaver, editors. Arctic Ecosystems in a Changing Climate: An Ecosphysiological Perspective. Academic Press, Inc., San Diego.

Tucker, C. J. 1979. Red and photographic infrared linear combinations for monitoring vegetation. Remote Sensing of Environment **8**:127-150.

Ustin, S. L., and J. A. Gamon. 2010. Remote sensing of plant functional types. New Phytol **186**:795-816.

Vierling, L. A., D. W. Deering, and T. F. Eck. 1997. Differences in arctic tundra vegetation type and phenology as seen using bidirectional radiometry in the early growing season. Remote Sensing of Environment **60**:71-82.

Vogelmann, J. E., and D. M. Moss. 1993. Spectral reflectance measurements in the genus Sphagnum. Remote Sensing of Environment **45**:273-279.

Walker, D., N. A. Auerbach, J. G. Bockheim, F. S. Chapin, W. Eugster, J. Y. King, J. P. McFadden, G. J. Michaelson, F. Nelson, W. C. Oechel, C. L. Ping, W. S. Reeburg, S. Regli, N. Shiklomanov, and G. L. Vourlitis. 1998. Energy and trace-gas fluxes across a soil pH boundary in the Arctic. Nature **394**.

Walker, D., N. A. Auerbach, and M. Shippert. 1995. NDVI, biomass, and landscape evolution of glaciated terrain in northern Alaska. Polar Record **31**:169-178.

Walker, D., J. G. Bockheim, F. S. Chapin, W. Eugster, F. Nelson, and C. L. Ping. 2001. Calcium-rich tundra, wildlife, and the "Mammoth Steppe". Quaternary Science Reviews **20**:149-163.

Walker, D., H. E. Epstein, V. E. Romanovsky, C. L. Ping, G. J. Michaelson, R. P. Daanen, Y. L. Shur, R. A. Peterson, W. B. Krantz, M. Raynolds, W. A. Gould, G. Gonzalez, D. J. Nicolsky, C. M. Vonlanthen, A. N. Kade, P. Kuss, A. M. Kelley, C. A. Munger, C. T. Tarnocai, N. V. Matveyeva, and F. J. A. Daniëls. 2008. Arctic patterned-ground ecosystems: A synthesis of field studies and models along a North American Arctic Transect. Journal of Geophysical Research **113**:1-17.

Walker, D., P. Kuss, H. E. Epstein, A. N. Kade, C. M. Vonlanthen, M. Raynolds, and F. J. A. Daniëls. 2011. Vegetation of zonal patterned-ground ecosystems along the North America Arctic bioclimate gradient. Applied Vegetation Science **14**:440-463.

Walker, D., M. Raynolds, F. J. A. Daniels, E. Einarsson, A. Elvebakk, W. A. Gould, A. E. Katenin, S. S. Kholod, C. J. Markon, and B. A. Yurstev. 2005. The Circumpolar Arctic vegetation map. Journal of Vegetation Science **16**:267-282.

Walker, D. A. 1999. An integrated vegetation mapping approach for northern Alaska (1:4 M scale). International Journal of Remote Sensing **20**:2895-2920.

Walker, D. A., H. E. Epstein, G. Jia, A. Balser, C. Copass, E. J. Edwards, W. A. Gould, J. Hollingsworth, J. A. Knudson, H. A. Maier, A. Moody, and M. K. Raynolds. 2003a. Phytomass, LAI, and NDVI in northern Alaska: Relationships to summer warmth, soil pH, plant functional types, and extrapolation to the circumpolar Arctic. Journal of Geophysical Research **108**.

Walker, D. A., H. E. Epstein, M. K. Raynolds, P. Kuss, M. A. Kopecky, G. V. Frost, F. J. A. Daniëls, M. O. Leibman, N. G. Moskalenko, G. V. Matyshak, O. V. Khitun, A. V. Khomutov, B. C. Forbes, U. S. Bhatt, A. N. Kade, C. M. Vonlanthen, and L. Tichý. 2012. Environment, vegetation and greenness (NDVI) along the North America and Eurasia Arctic transects. Environmental Research Letters **7**:015504.

Walker, D. A., G. J. Jia, H. E. Epstein, M. K. Raynolds, F. S. Chapin Iii, C. Copass, L. D. Hinzman, J. A. Knudson, H. A. Maier, G. J. Michaelson, F. Nelson, C. L. Ping, V. E. Romanovsky, and N. Shiklomanov. 2003b. Vegetation-soil-thaw-depth relationships along a low-arctic bioclimate gradient, Alaska: synthesis of information from the ATLAS studies. Permafrost and Periglacial Processes **14**:103-123.

Walker, M. D., D. Walker, and N. A. Auerbach. 1994. Plant communities of a tussock tundra landscape in the Brooks Range Foothills, Alaska. Journal of Vegetation Science **5**:843-866.

Winton, M. 2006. Amplified Arctic climate change: What does surface albedo feedback have to do with it? Geophysical Research Letters **33**.

Xu, H., T. Twine, and X. Yang. 2014. Evaluating Remotely Sensed Phenological Metrics in a Dynamic Ecosystem Model. Remote Sensing **6**:4660-4686.

Zeng, H., G. Jia, and H. Epstein. 2011. Recent changes in phenology over the northern high latitudes detected from multi-satellite data. Environmental Research Letters **6**:045508.

Chapter 2: Relationships between hyperspectral data and components of vegetation biomass in Low Arctic tundra communities at Ivotuk, Alaska

1. Abstract

Warming in the Arctic has resulted in a lengthening of the growing season and changes to the distribution and composition of tundra vegetation including increased biomass quantities in the Low Arctic. Biomass has commonly been estimated using broad-band greenness indices such as Normalized Difference Vegetation Index (NDVI); however, vegetation changes in the Arctic are occurring at spatial scales within a few meters and may not be uniquely identifiable using broad-band indices. The aim of this chapter is to assess the ability of hyperspectral remote sensing data to estimate biomass quantities among different plant tissue type categories at the North Slope site of Ivotuk, Alaska. Hand-held hyperspectral data and harvested biomass measurements were collected during the 1999 growing season. A subset of the data was regressed against hyperspectral bands using LASSO regression. The resulting model was then used to predict biomass quantities for the remaining Ivotuk data. The majority of significant biomass-spectra relationships (65%) were for shrubs categories during all times of the growing season. Biomass-spectra relationships relied most heavily on bands in the blue, green, and red edge regions of the spectrum. The ability to identify unique biomass-spectra relationships per community is decreased at the height of the growing season when shrubs obscure lower-lying vegetation such as mosses. The results of this study support previous research arguing that shrubs are dominant controls over spectral reflectance in Low Arctic communities and that this dominance results in an increased ability to estimate shrub component biomass over other plant functional types.

2. Introduction

The Arctic has warmed at a greater rate than the rest of the globe through a process known as polar amplification (Serreze and Francis 2006, Winton 2006, Walker et al. 2012). Global change in temperature from 1981-2012 was estimated to be 0.17°C per decade (Hansen et al. 2010), while warming in the Arctic (>66°N) has been approximately 0.60 ± 0.07°C per decade (Comiso and Hall 2014) over the past century. Remotely sensed land surface temperature (LST) data from 1982-2008 indicate warming to be greater in the North American Arctic (+30%) than in the Eurasian Arctic (+16%) based on the Summer Warmth Index (SWI), which is the sum of average monthly surface temperatures above freezing (Bhatt et al. 2010). Temperature increases have had probable effects on tundra ecosystems, such as a lengthening of the growing season (Huemmrich et al. 2010b, Zeng et al. 2011), and associated increases in vegetation biomass; the Alaskan arctic tundra biomass has increased on average by 7.8% since the early 1980s (Epstein et al. 2012).

Vascular and non-vascular (i.e. mosses and lichens) vegetation may respond differently to climate change (Huemmrich et al. 2013). Mosses and lichens are often abundant in tundra ecosystems, though warming trends have led to atypical increases in vascular plant cover (Huemmrich et al. 2013) and decreases in non-vascular cover (Walker et al. 2006). This trend is not evident in all regions of the Arctic, and the High Arctic and alpine tundra have not experienced the same increases in vascular plant coverage (Cornelissen et al. 2001). The observed increases in shrub abundance throughout the Low Arctic tundra (Myers-Smith et al. 2011) may be due to their ability to outcompete other vegetation types, potentially through shading of non-vascular species (Chapin et al. 1995, Cornelissen et al. 2001, Sturm et al. 2001a).

Remote sensing has allowed scientists to monitor changes occurring in arctic vegetation at a variety of spatial and temporal scales (Stow et al. 2004). Past studies have mapped changes

in vegetation using aerial photography (Sturm et al. 2005), coarse-scale satellite imagery such as that from the Advanced Very High Resolution Radiometer (AVHRR) (Walker 1999), and moderate-scale satellite imagery such as that from Landsat platforms (Muller et al. 1999, Silapaswan et al. 2001). Though vegetation change in the Arctic occurs on fine spatial scales with changes in individual plant types, the use of high-resolution and hyperspectral imagery remains scarce (however, see Forbes et al. 2010, Buchhorn et al. 2013, Huemmrich et al. 2013). Hyperspectral remote sensing allows for the use of information contained in more refined regions of the spectrum than might be obscured with broad-band data. This may be useful for identifying otherwise unobservable differences in vegetation structure and biochemical composition among plant tissue types in the Arctic.

Past studies have developed estimates of arctic tundra biomass using relationships with environmental factors (including other vegetation variables), such as SWI, gross primary productivity (GPP), and leaf area index (LAI) using simple regression (Riedel et al. 2005a, Riedel et al. 2005b, Epstein et al. 2008, Walker et al. 2012, van der Wal and Stien 2014) and multiple regression analyses (Ueyama et al. 2013). Multiple studies have developed relationships between arctic tundra biomass and the remotely sensed Normalized Difference Vegetation Index (NDVI - (e.g. Hope et al. 1993, Walker 2003, Stow et al. 2004, Riedel et al. 2005b, Raynolds et al. 2012). Shrubs contribute substantially to NDVI in the most southern areas of the arctic tundra (Figure 2.1), whereas bryophytes contribute relatively more to NDVI in the more northern subzones, where shrub cover is sparse (Raynolds et al. 2012). Shrubs may become a more important component of tundra plant community biomass, as their cover and abundance increase with warmer temperatures (Walker et al. 1995, Riedel et al. 2005b).

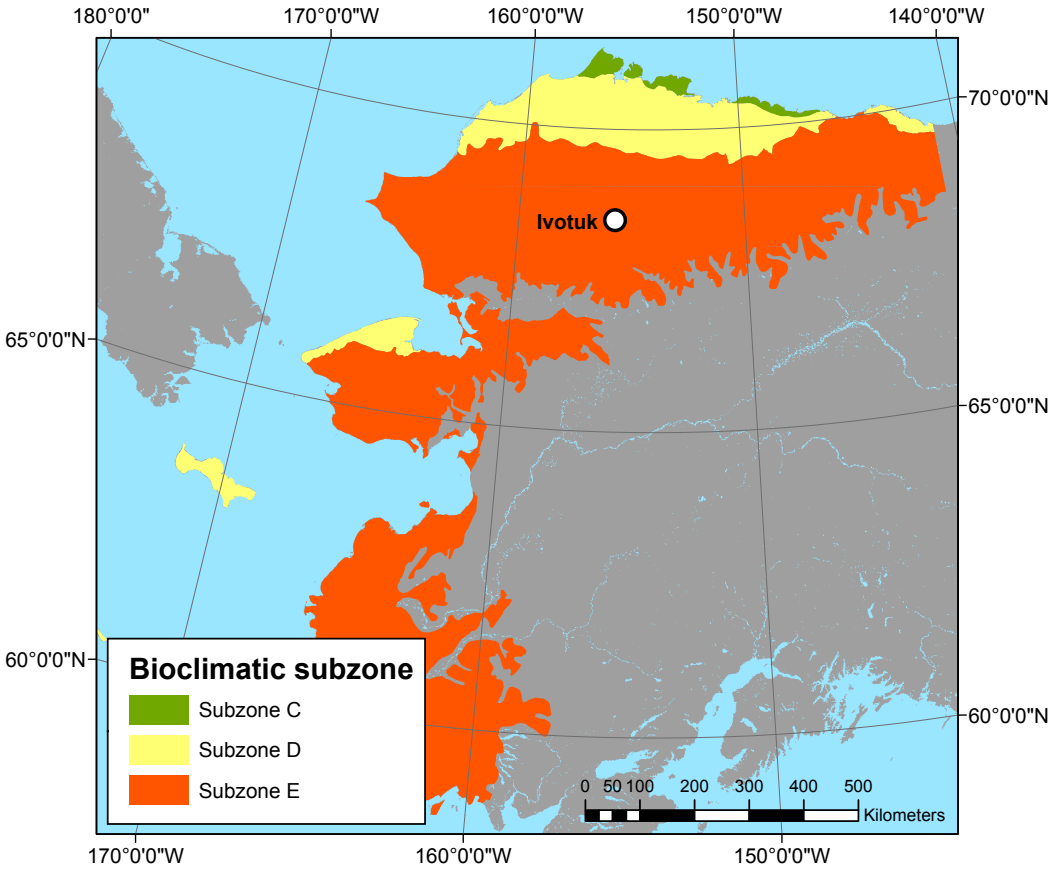

Figure 2.1. Location of Ivotuk on the North Slope of Alaska within the Alaskan bioclimatic subzones of the Circumpolar Arctic Vegetation Map (CAVM 2003).

Establishing relationships between plant tissue type biomass and hyperspectral information may be extremely useful for tracking changes in arctic biomass occurring with increasing temperatures. Different regions of the visible and near infrared spectra can be used to identify functional and structural properties of vegetation communities and individual plant tissue types (Curran 1989, Ustin and Gamon 2010). Hyperspectral remote sensing (also known as imaging spectroscopy) has been useful in differentiating among vascular and non-vascular vegetation (Huemmrich et al. 2013) and functionally distinct vegetation types in the Arctic (Buchhorn et al. 2013). Moss and vascular plant spectra have similar reflectances in the green and near infrared (NIR) wavelengths, whereas lichens have higher reflectance in the visible, and

greater variability in species-specific reflectances (Huemmrich et al. 2013). Dead biomass in the Arctic also influences the reflectivity spectra, particularly as shrubs begin to dominate these systems, and their leaf litter covers more low-lying plants (DeMarco et al. 2014, Xu et al. 2014). Narrow-band NDVI combinations have been used in addition to broad-band NDVI measurements, and show slightly better correlations with biomass (Buchhorn et al. 2013). However, to date, hyperspectral data have not been evaluated for their utility in improving remotely sensed estimates of tundra biomass. The goal of this research was therefore to establish relationships between tundra biomass components and hyperspectral data from a Low Arctic site in Alaska using handheld hyperspectral remote sensing.

3. Methods

3.1 Study Area

Ivotuk, Alaska (68.49°N, 155.74°W) is located on the North Slope of the Brooks Mountain Range (Epstein et al. 2004b, Riedel et al. 2005a, Riedel et al. 2005b), and was one of seven sites established as part of the Arctic Transitions in the Land-Atmosphere System (ATLAS) project (McGuire 2003, Walker et al. 2003a, Walker et al. 2003b). Ivotuk is part of the Western Alaska Transect that starts in the north at Barrow and goes south through Atqasuk and Oumalik to Ivotuk (Jia et al. 2002, McGuire 2003, Walker et al. 2003a, Epstein et al. 2008). The Eastern Alaska Transect starts in the north at Prudhoe Bay and ends at Toolik Lake, a Long-Term Ecological Research (LTER) site (Walker et al. 1994, Chapin et al. 1995, Hobbie et al. 1999). Ivotuk is located in bioclimatic subzone E (Figure 2.1), which includes the Arctic Foothills and non-forested areas of the Seward Peninsula (Walker et al. 2003b). The CAVM identifies five bioclimatic subzones (A-E) based on differences in climate, vegetation, topography, substrate biogeochemistry, and NDVI (CAVM 2003, Walker et al. 2005, Raynolds et al. 2006). Subzone E is the southernmost and warmest of the five tundra subzones. Ivotuk is largely a tussock tundra ecosystem also dominated by deciduous shrubs (Walker et al. 2003a). It is located at an elevation of approximately 550m (Epstein et al. 2004b). From 1991-2001 (a time period that encompasses the sampling that will be used for this research), the site received an annual average of 202 mm precipitation, had a July maximum temperature of approximately 12°C, an annual temperature of -10.9°C, and a 110-day growing season (Jia et al. 2002, Riedel et al. 2005a, Riedel et al. 2005b).

The site of Ivotuk is comprised of the four plant communities of moist acidic tundra (MAT), moist nonacidic tundra (MNT), mossy tussock tundra (MT) and shrub tundra (ST). MAT and MNT are differentiated by soil acidity, with MAT occurring on soils with pH < 5.0-5.5, and

MNT occurring on soils with pH ≥ 5.0-5.5 (Walker et al. 1994, Walker et al. 2003a). MAT, also referred to as tussock-graminoid tundra, is dominated by dwarf erect shrub species such as *Betula nana*, and the tussock sedge *Eriophorum vaginatum* (Walker et al. 1994). *Betula nana* is absent in MNT due to low soil acidity. Mosses, graminoids, non-tussock sedges, and prostrate dwarf shrubs such as *Dryas integrifolia* dominate in MNT communities (Walker et al. 1994, Jia et al. 2004). MT contributes greatly to biomass quantities in tundra systems, and is typified as an acidic tussock tundra with abundant *Sphagnum* mosses (Tenhunen et al. 1992). ST is dominated by shrubs such as *Salix alaxensis, Betula nana,* and *Alnus crispa* (Muller et al. 1999), and is interspersed with graminoids, forbs, lichens, and mosses.

3.2 Species Composition

Species data were collected in 1999 using the Braun-Blanquet method (Westhoff and van der Meel 1973). Mosses were one of the most abundant plant functional types in all four communities (Table 2.1). *Hylocomium splendens* (51-75%) was the most common in MAT, as well as in ST, where the deciduous shrub *Rubus chamaemorus* also dominates species composition (51-75%). The moss *Tomentypnum nitens*, (26-50%), the evergreen shrub *Dryas integrifolia*, and the graminoid *Carex bigelowii* all occurred with a frequency of (26-50%) in MNT. Graminoids were the most abundant PFT in MT, with the largest contributor as the species *Eriophorum vaginatum* (51-75%).

Table 2.1. Dominant plant species at Ivotuk, Alaska per plant vegetation community and plant functional type. Species are presented along with their Braun-Blanquet percentages. Most abundant species are shown in gray.

PLANT FUNCTIONAL TYPE	VEGETATION COMMUNITY			
	MAT	MNT	MT	ST

Deciduous shrub	*Betula nana* ssp. *exilis* (26-50%)	*Salix reticulata* (6-25%)	*Rubus chamaemorus* (6-25%)	*Rubus chamaemorus* (51-75%)
Evergreen shrub	*Rhododendron tomentosum* subsp. *decumbens* (26-50%)	*Dryas integrifolia* (26-50%)	*Rhododendron tomentosum* subsp. *decumbens* (6-25%)	*Pyrola grandiflora* (1-5%)
Forb	*Petasites frigidus* (6-25%)	*Geum glaciale* (6-25%)	--	*Petasites frigidus* (26-50%)
Graminoid	*Eriophorum vaginatum* (26-50%)	*Carex bigelowii* (26-50%)	*Eriophorum vaginatum* (51-75%)	*Eriophorum angustifolia* (26-50%)
Lichen	*Baeomyces carneus*, & *Peltigera aphthosa* (1-5%)	*Thamnolia vermicularis* s. *subuliformis* (6-25%)	*Cladonia amaurocraea*, *C. arbuscula*, *C. stygia*, *Dactylina arctica*, *Flavocetraria cucullata*, *Peltigera rufescens*, and *Thamnolia vermicularis* var. *subuliformis* (0.5%)	*Peltigera leucophlebia* (1-5%)
Moss	*Hylocomium splendens* (51-75%)	*Tomentypnum nitens* (26-50%)	*Sphagnum lenense* (26-50%)	*Hylocomium splendens* (51-75%)

3.3 Data Collection and Processing

One 100 m x 100 m grid was established in each of the four vegetation communities (Walker et al. 2003a, Walker et al. 2003b, Riedel et al. 2005a, Riedel et al. 2005b, Epstein et al. 2008). Spectroscopy data were collected during the 1999 growing season at biweekly intervals from 5 June - 26 August and grouped according to early, peak, and late growing season (Table 2.2). Late growing season was excluded from this analysis due to a limited number of observations. Spectral measurements were made using an Analytical Spectral Devices FieldSpec spectro-radiometer with a spectral resolution of 1.42 nm and a spectral range of 330.79-1061.78 nm

(Riedel et al. 2005a, Riedel et al. 2005b). Spectral measurements were collected from ten random gridpoints established in each of the four vegetation grids. Biomass data were also collected biweekly from ten 20 x 50 cm plots adjacent to these spectral gridpoints (Walker et al. 2003a, Epstein et al. 2004b, Riedel et al. 2005a, Riedel et al. 2005b, Epstein et al. 2008). Both biomass and spectral measurements were collected from an additional ten gridpoints during one sampling period within peak growing season (Riedel et al. 2005a, Riedel et al. 2005b).

Vascular plants were clipped at the top of the moss surface, and mosses were clipped at the base of the green layer (Walker et al. 2003a, Epstein et al. 2004b, Riedel et al. 2005a, Riedel et al. 2005b). Biomass samples were sorted into seven functional categories including evergreen and deciduous shrubs, graminoids, horsetails, other forbs (hereafter simply "forbs"), bryophytes, and lichens (Walker et al. 2003a, Riedel et al. 2005a, Riedel et al. 2005b). Samples were oven-dried at 55°C for 48 hours before being taken back to the University of Virginia for further processing (Epstein et al. 2004b). Graminoids were divided into live and dead materials (Riedel et al. 2005a, Riedel et al. 2005b). Evergreen and deciduous shrubs were divided into woody, foliar live, and foliar dead materials (Epstein et al. 2004b, Riedel et al. 2005a, Riedel et al. 2005b).

Table 2.2. Biomass sampling dates and observation count per vegetation community during the 1999 growing season.

Growing season	MAT	MNT	MT	ST
Early	5 June-3 July (*n* = 22)	8 June-10 July (*n* = 20)	10 June-9 July (*n* = 20)	6 June-11 July (*n* = 20)
Peak	13 July-14 August (*n* = 28)	25 July-22 August (*n* = 33)	16 July-24 August (*n* =24)	26 July-23 August (*n* = 20)

3.4 Spectral Processing

Original field spectroscopy data from Ivotuk were resampled to 5 nm wide hyperspectral narrowbands (HNBs) ranging from 400-1000 nm. Resampling increases the signal-to-noise ratio (SNR), reduces wavelength redundancy issues, and makes results more interpretable and comparable to other Alaska sites for which handheld data may have been taken in different wavebands, or to hyperspectral satellites with different wavebands. As a quality assurance step, reflectance spectra from Ivotuk were examined visually for irregularities. Irregular spectra were removed before analysis in an effort to overcome the heterogeneous nature of vegetation at Ivotuk and develop a more diagnostic spectral signature.

3.5 Data Analysis

Regularization methods such as the least absolute shrinkage and selection operator (LASSO) are valuable tools for addressing many of the analytical problems affecting hyperspectral remote sensing such as high collinearity. LASSO is a modified form of partial least squares regression that reduces model complexity using a regularization parameter and is unaffected by the order of variable entry into a model (Tibshirani 1996). The regularization parameter works by shrinking variable coefficients toward zero, and eliminating variables from the model when their coefficients reach zero. As such, LASSO is an effective variable selection and dimensionality reduction technique.

Data were first analyzed without separation by vegetation community, meaning that all biomass data from either early or peak season for all four vegetation types were used for analysis. This was then repeated with community separation (i.e. within vegetation type) in order to establish relationships between biomass categories and spectral variables specific to a vegetation community. Sample size per vegetation community ranged from 20-22 during early

growing season and from 20-33 during peak growing season (Table 2.2). A simple random sample of one-half of the Ivotuk data was used to create the training set. The remaining one-half was used to create the test set. Plant tissue type biomass quantities were then regressed against spectra using LASSO regression from the "glmnet" package in R (Friedman et al. 2010).

4. Results

4.1 Early Growing Season – Without Separation by Vegetation Community Type

Total biomass across all four vegetation communities during early growing season was 768.9 g/m^2. The greatest contributor to live biomass was moss (306.9 g/m^2), followed by deciduous shrub (183.6 g/m^2), evergreen shrub (61.9 g/m^2), graminoid (37.1 g/m^2), lichen (22.2 g/m^2), and forb (8.7 g/m^2) (Figure 2.2). The best relationships between plant tissue type and spectral reflectances were for deciduous shrub-live foliar and shrub total-live (adjusted $r^2 = 0.44$) (Figure 2.3). Other significant relationships included evergreen shrub-woody (adjusted $r^2 = 0.43$), deciduous shrub-woody (adjusted $r^2 = 0.40$), shrub total (adjusted $r^2 = 0.39$), deciduous shrub-dead foliar (adjusted $r^2 = 0.33$), and total-live (adjusted $r^2 = 0.31$) (Table 2.3).

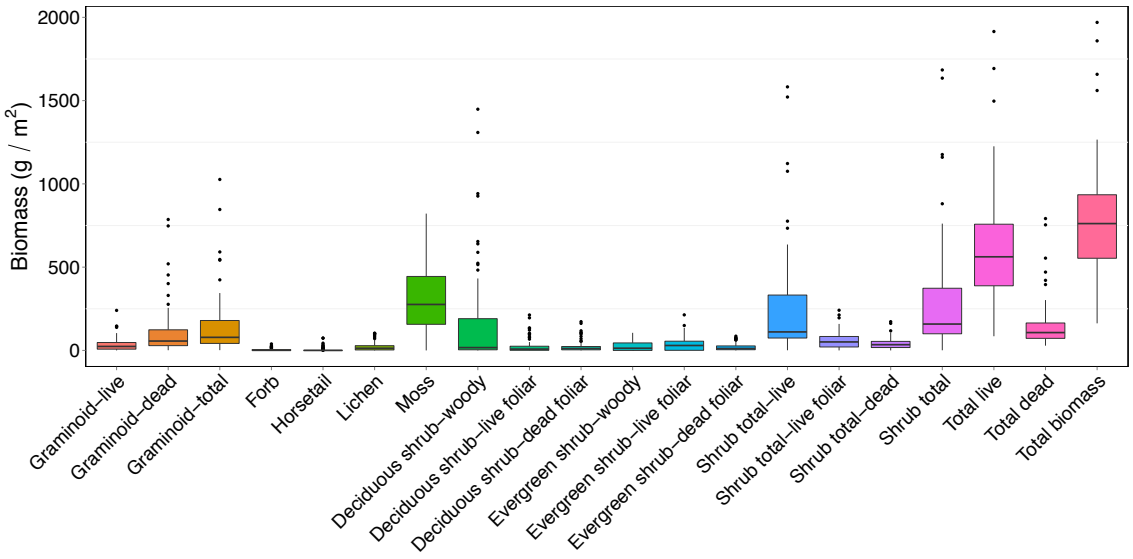

Figure 2.2. Range of biomass quantities per plant tissue type during early growing season at Ivotuk, Alaska without separation by vegetation community

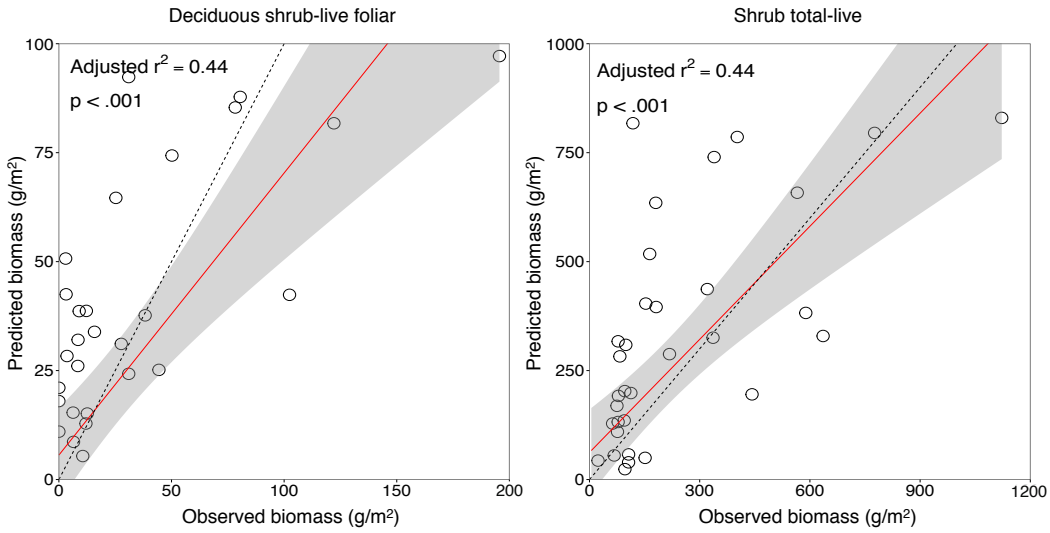

Figure 2.3. Best relationships between plant tissue type biomass components during early growing season without separation by vegetation community. The top relationships were for deciduous shrub-live foliar and shrub total-live. The solid red line represents the best-fit line, and the dashed line is the 1:1 line.

Table 2.3. Significant relationships during early growing season without separation by vegetation community

Plant Tissue Type	Predictor Bands	Adjusted r-square	p
Deciduous shrub-live foliar	435, 440, 450, 520, 560, 565, 665, 860, 990, 995	0.44	< .001
Shrub total-live	405, 450, 570, 665, 680, 710, 845, 850, 855, 990	0.44	< .001
Evergreen shrub-woody	400, 440, 555, 560, 730, 765, 1000	0.43	< .001
Deciduous shrub-woody	405, 450, 570, 660, 665, 855, 870, 990	0.40	< .001
Shrub total	405, 445, 450, 570, 665, 680, 710, 845, 850, 855, 990	0.39	< .001

Deciduous shrub-dead foliar	405, 475, 495, 540, 545, 570, 665, 685, 690, 695, 720, 850, 865, 880, 895, 965, 970, 990	0.33	< .001
Total-live	445, 885, 890	0.31	< .001

4.2 Early Growing Season – With Separation by Vegetation Community Type

Shrub tundra had the greatest total biomass during early growing season (1063.3 g/m^2), followed by MAT (683.5 g/m^2), MT (679.6 g/m^2), and MNT (657.9 g/m^2) (Figure 2.4). The plant tissue type that contributed the most biomass to MAT was graminoid-dead (173.6 g/m^2). Moss was the greatest contributor in both MNT (462.5 g/m^2) and MT (288.4 g/m^2). Deciduous shrub-woody was the greatest contributor in ST (542.7 g/m^2). The best relationship between biomass and spectral reflectances in MAT was for evergreen shrub-live foliar (adjusted $r^2 = 0.62$) (Figure 2.5). MAT also had significant relationships with shrub total-live foliar (adjusted $r^2 = 0.56$), shrub total-live (adjusted $r^2 = 0.33$), and total-live (adjusted $r^2 = 0.33$) (Table 2.4). MNT had two significant relationships with shrub total-live foliar and shrub total-live (adjusted $r^2 = 0.33$). MT had no significant relationships. The best relationship for ST was for shrub total-live foliar (adjusted $r^2 = 0.61$). ST also had significant relationships with graminoid-total (adjusted $r^2 = 0.59$) and deciduous shrub-live foliar (adjusted $r^2 = 0.46$).

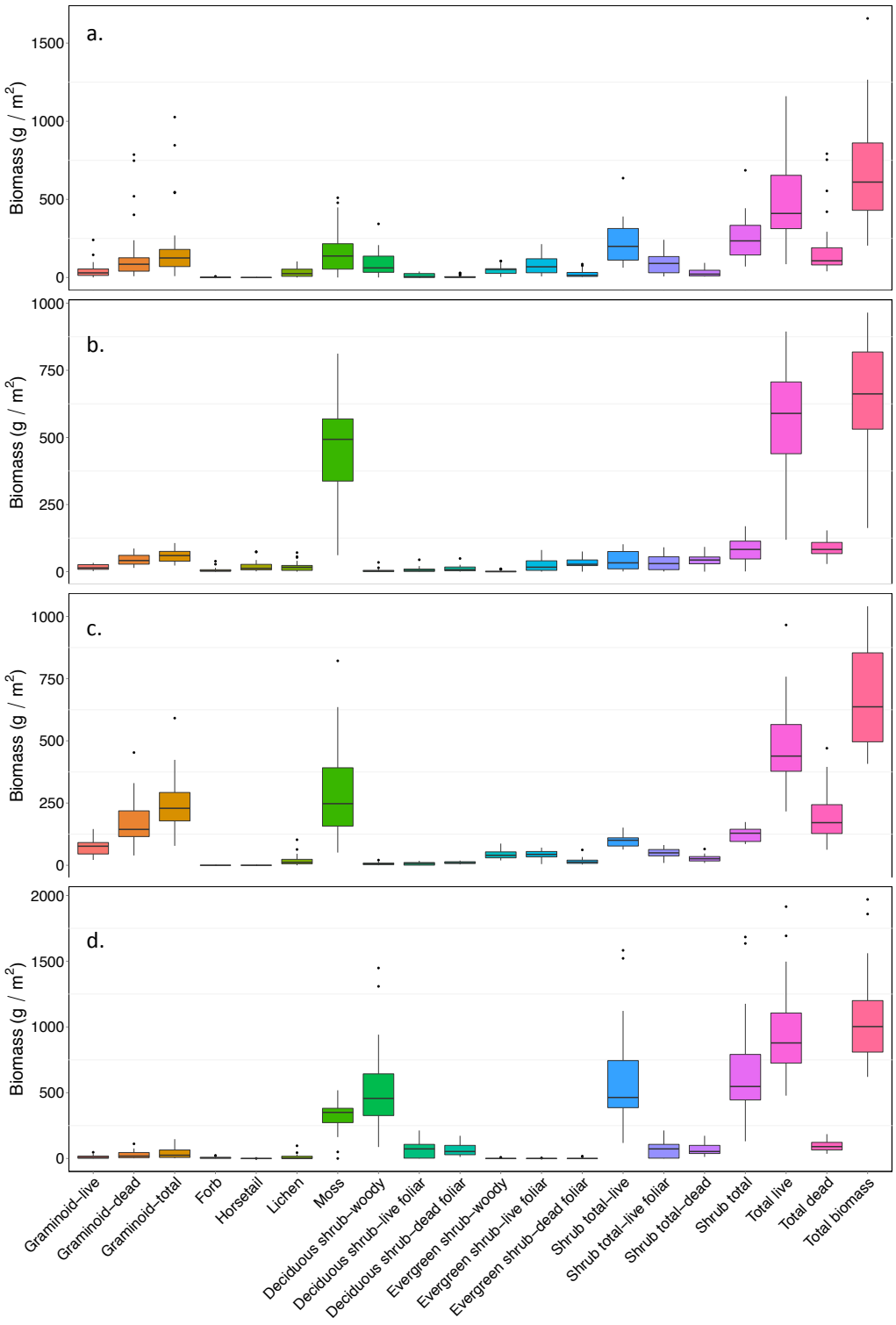

Figure 2.4. Biomass quantity per plant tissue type biomass component during early growing season for vegetation communities of MAT (a), MNT (b), MT (c), ST (d) at Ivotuk, Alaska

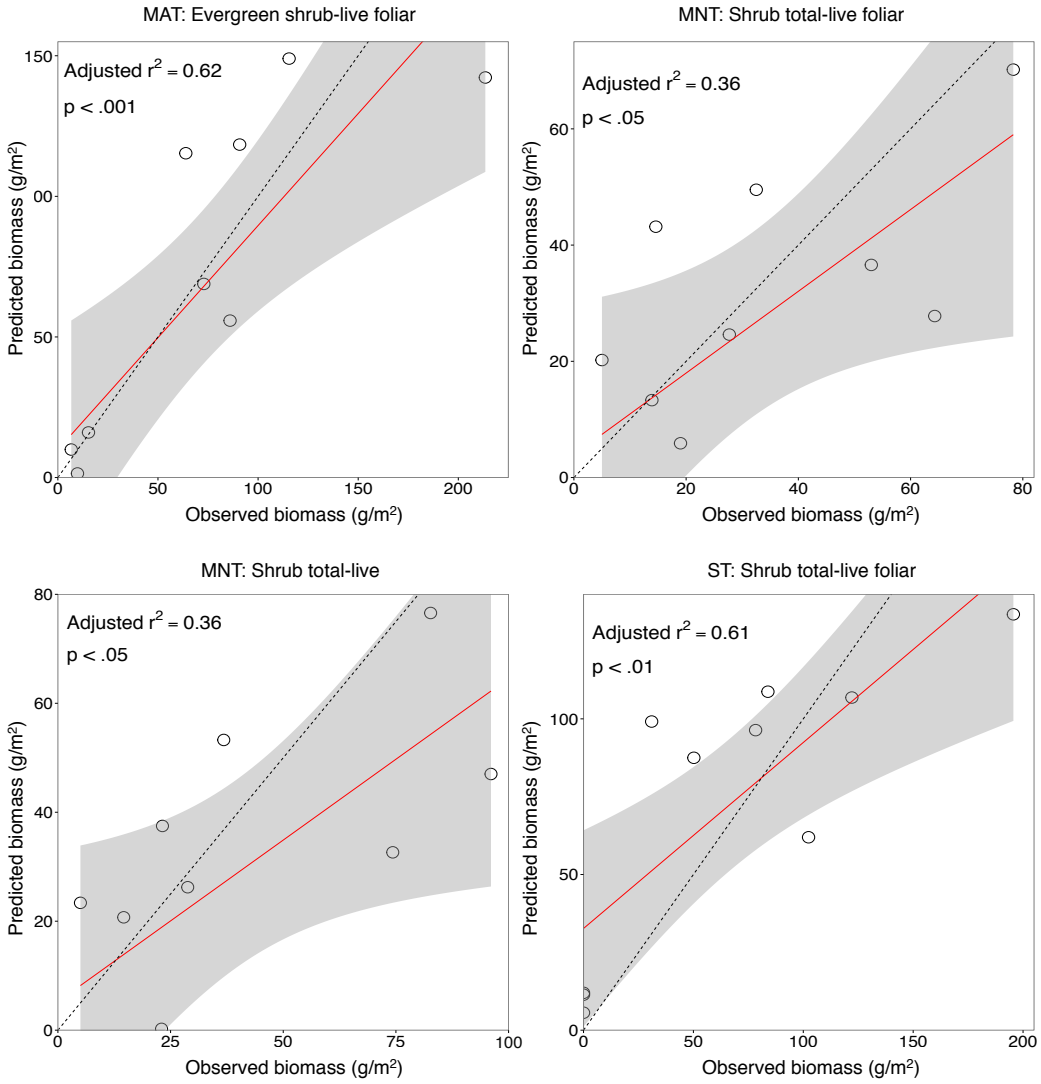

Figure 2.5. Relationship between plant tissue type biomass components during early growing season for four vegetation communities at Ivotuk, Alaska. Best relationships were for MAT and evergreen shrub-live foliar, MNT shrub total-live foliar and shrub total-live, and ST and shrub total-live foliar. The solid red line represents the best fit line, and the dashed line is the 1:1 line.

Table 2.4. Significant relationships during early growing season for four vegetation communities at Ivotuk, Alaska

Community	Plant Tissue Type	Predictor Bands	Adjusted r-square	p
MAT	Evergreen shrub-live foliar	420, 490, 540, 560, 565, 705	0.62	< .001
MAT	Shrub total-live foliar	695, 700	0.56	< .01
MAT	Shrub total-live	700	0.33	< .05
MAT	Total-live	670, 675,	0.33	< .05
MNT	Shrub total-live foliar	435, 680, 705, 710, 740, 1000	0.36	< .05
MNT	Shrub total-live	435, 580, 605, 680, 705, 1000	0.36	< .05
ST	Shrub total-live foliar	675, 730, 735	0.61	< .01
ST	Graminoid-total	475, 480, 710, 715, 980	0.59	< .01
ST	Deciduous shrub-live foliar	495, 500, 510, 555	0.46	< .05

4.3 Spectra during early growing season – without community separation

The majority of hyperspectral narrow bands (HNBs) present in the biomass-spectra relationships for early growing season and without separation by community type were in the near infrared wavelength region (Figure 2.6). The next most common wavelength region was the blue followed by the near infrared plateau and green, the red edge and yellow, and the least common wavelength region was red. No relationships used bands in the orange wavelength region of the

spectrum. While the majority of HNBs used is present in the near infrared, those in the blue and green wavelength regions load more highly, and therefore more significantly affect the biomass-spectra relationships. Those in the yellow, orange, and red load more highly than those in the near infrared and near infrared plateau.

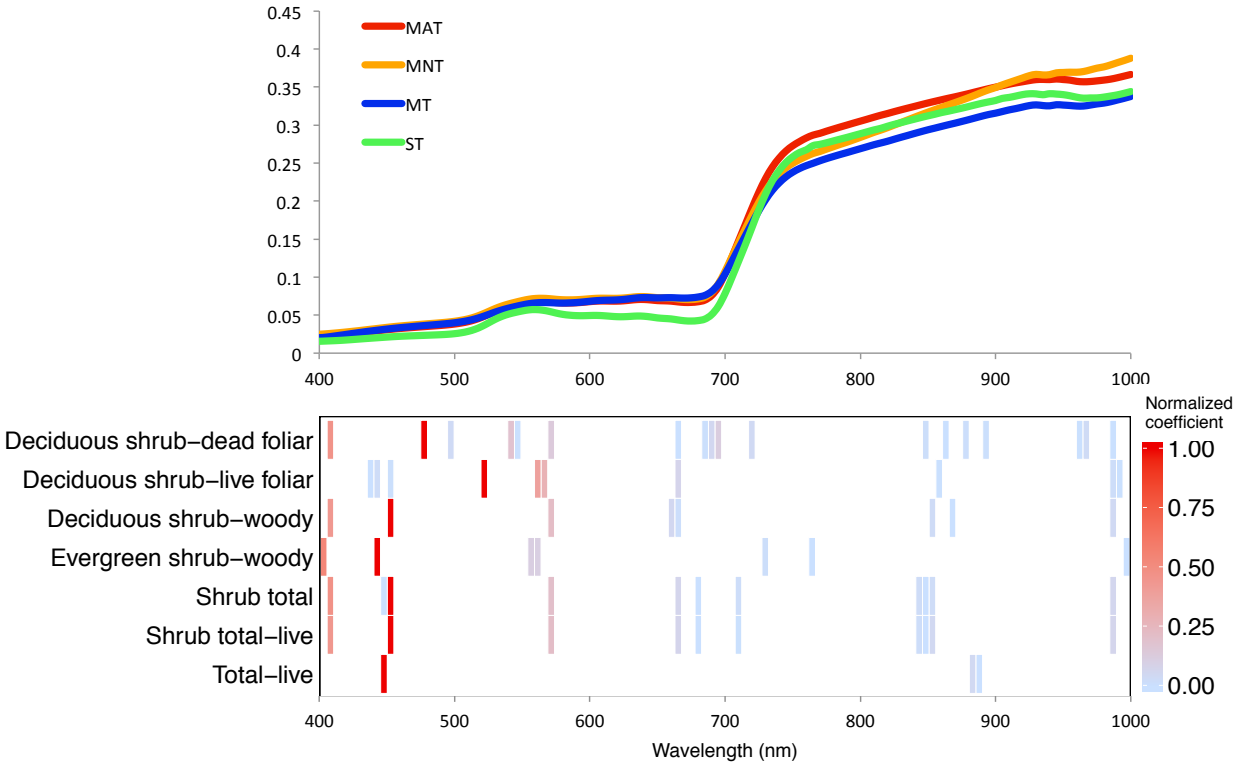

Figure 2.6. Mean reflectance for all vegetation communities during early growing season along with the normalized coefficients for the optimal HNBs associated with the plant tissue type categories for total biomass.

4.4 Spectra during early growing season – with community separation

The majority of HNBs for early growing season with separation by vegetation community type were located in the red edge (Figure 2.7). The next most common region of the spectrum was the green, followed by red, then blue, yellow, the near infrared, the near infrared plateau, and finally

orange. Bands in the red edge were dominant in MAT and MNT, while bands in the green wavelengths were dominant in ST. Bands in the red and red edge loaded highly in MAT, with bands in the blue and green loading highly for the relationship between MAT spectra and evergreen shrub-live foliar only. Bands in the red edge and the blue loaded highly for MNT, and bands in the green and red loaded highly in ST.

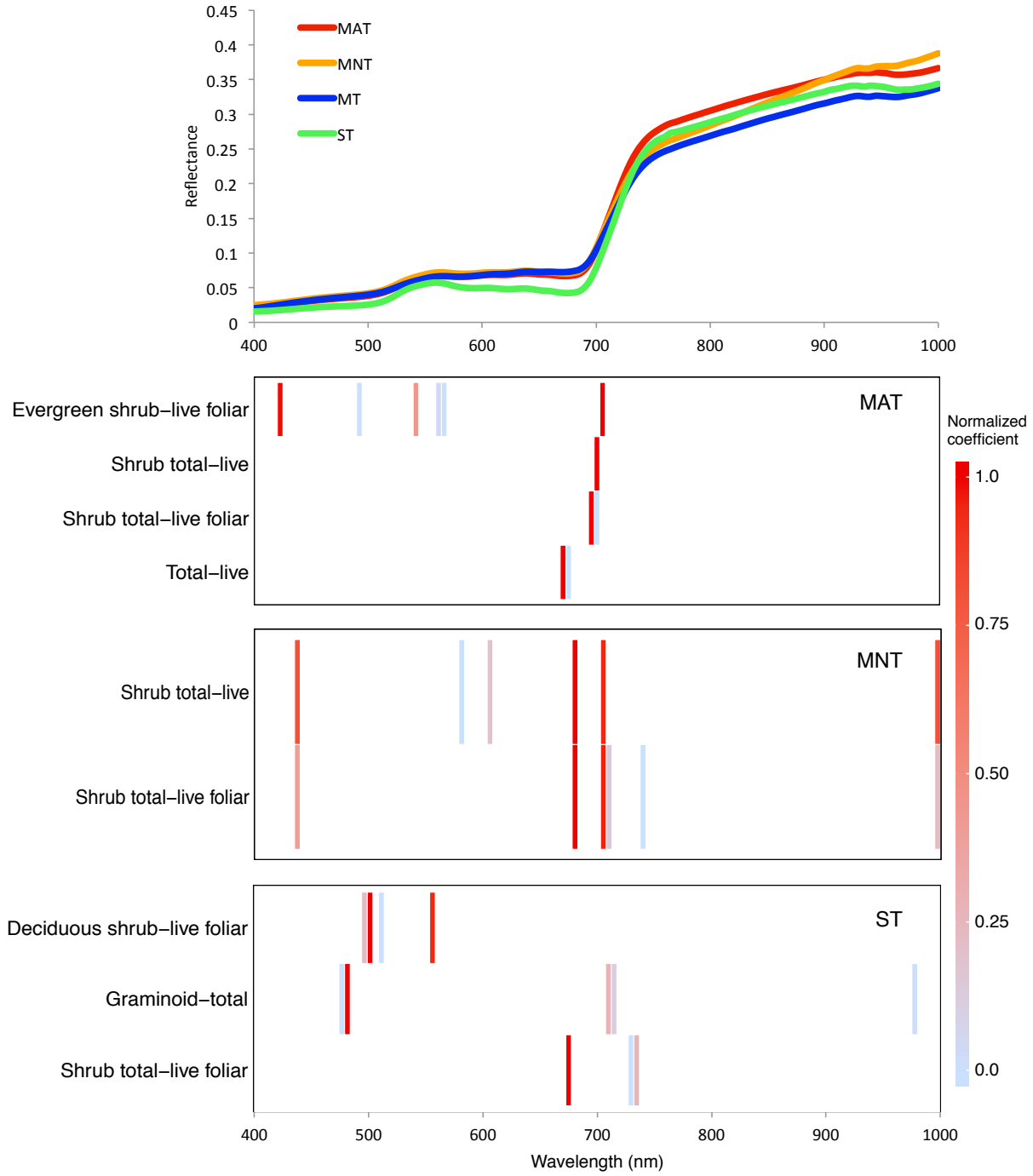

Figure 2.7. Mean reflectance for all vegetation communities during early growing season along with the normalized coefficients for the optimal HNBs associated with the plant tissue type categories for biomass per vegetation communities. There were no significant relationships for MT.

4.5 Peak Growing Season – Without Separation by Vegetation Community Type

Total biomass for all four vegetation communities during peak growing season was 851.2 g/m^2 (Figure 2.6). The greatest contributor to live biomass was moss (333.2 g/m^2), followed by deciduous shrubs (155.0 g/m^2), evergreen shrubs (89.0 g/m^2), graminoid (58.8 g/m^2), lichen (32.2 g/m^2), and forb (10.8 g/m^2) (Figure 2.8). The best relationship during peak growing season without separation by vegetation community type was for shrub total-live (adjusted $r^2 = 0.65$) (Figure 2.9). Peak growing season spectra were also related to the plant tissue type categories of deciduous shrub-woody (adjusted $r^2 = 0.64$), shrub total (adjusted $r^2 = 0.63$), deciduous shrub-live foliar (adjusted $r^2 = 0.39$), and deciduous shrub-dead foliar (adjusted $r^2 = 0.32$) (Table 2.5).

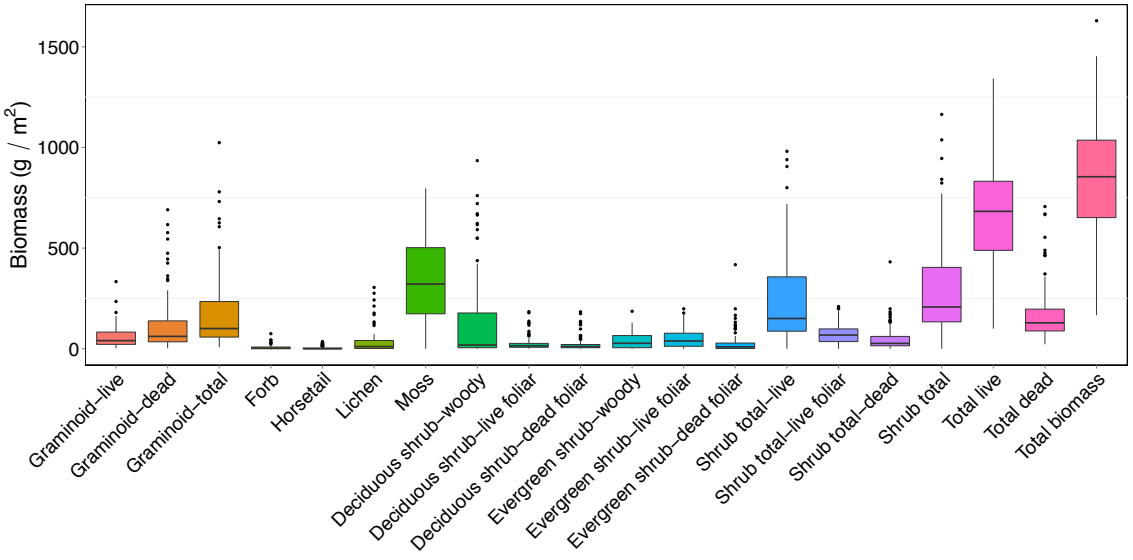

Figure 2.8. Biomass quantity per plant tissue type biomass component during peak growing season at Ivotuk, Alaska

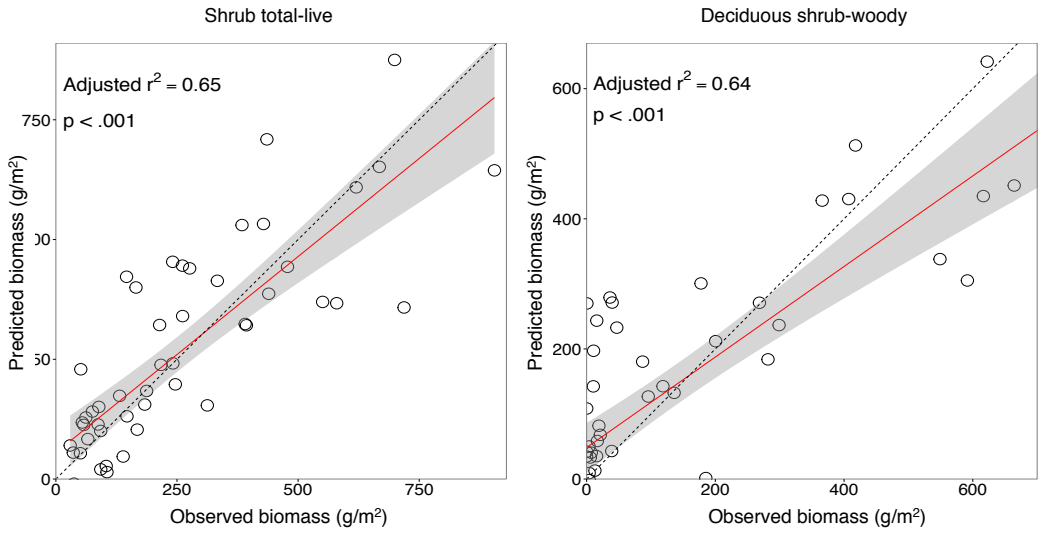

Figure 2.9. Relationship between plant tissue type and spectra during peak growing season without separation by vegetation community. Best relationships were for shrub total-live and deciduous shrub-woody. The solid red line represents the best-fit line, and the dashed line is the 1:1 line.

Table 2.5. Significant relationships for plant tissue types during peak growing season without separation by vegetation community

Plant Tissue Type	Predictor Bands	Adjusted r-square	p
Shrub total-live	400, 485, 490, 530, 590, 595, 690,695 715, 765, 985, 995, 1000	0.65	< .001
Deciduous shrub-woody	400, 485, 490, 535, 600, 605, 695, 715, 825, 855, 860, 940	0.64	< .001
Shrub total	400, 485, 490, 695, 715, 800, 805, 810, 825, 840, 845, 985	0.63	< .001
Deciduous shrub-live foliar	490, 670, 940	0.39	< .001
Deciduous shrub-dead foliar	485	0.32	< .001

4.6 Peak Growing Season – Separation by Vegetation Community Type

ST had the greatest total quantity of biomass during peak growing season (1129.1 g/m^2), followed by MAT (842.2 g/m^2), MT (815.2 g/m^2), and MNT (724.8 g/m^2) (Figure 2.10). The largest plant tissue type biomass contributor was moss in all communities except ST, at 201.5 g/m^2 in MAT, 445.8 g/m^2 in MNT, and 349.7 g/m^2 in MT. Deciduous shrub-woody was the greatest contributor in ST at 498.3 g/m^2. MAT had no significant relationships to plant tissue type biomass components during peak growing season. The most significant plant tissue type relationship in MNT was for evergreen shrub-dead foliar (adjusted $r^2 = 0.48$) (Figure 2.11). MNT also had a significant relationship with shrub total-dead (adjusted $r^2 = 0.45$). Spectral reflectances for MT were related to the two categories of total biomass (adjusted $r^2 = 0.42$), and moss (adjusted $r^2 = 0.36$). ST had a significant relationship for deciduous shrub-live foliar (adjusted $r^2 = 0.44$) only (Table 2.6).

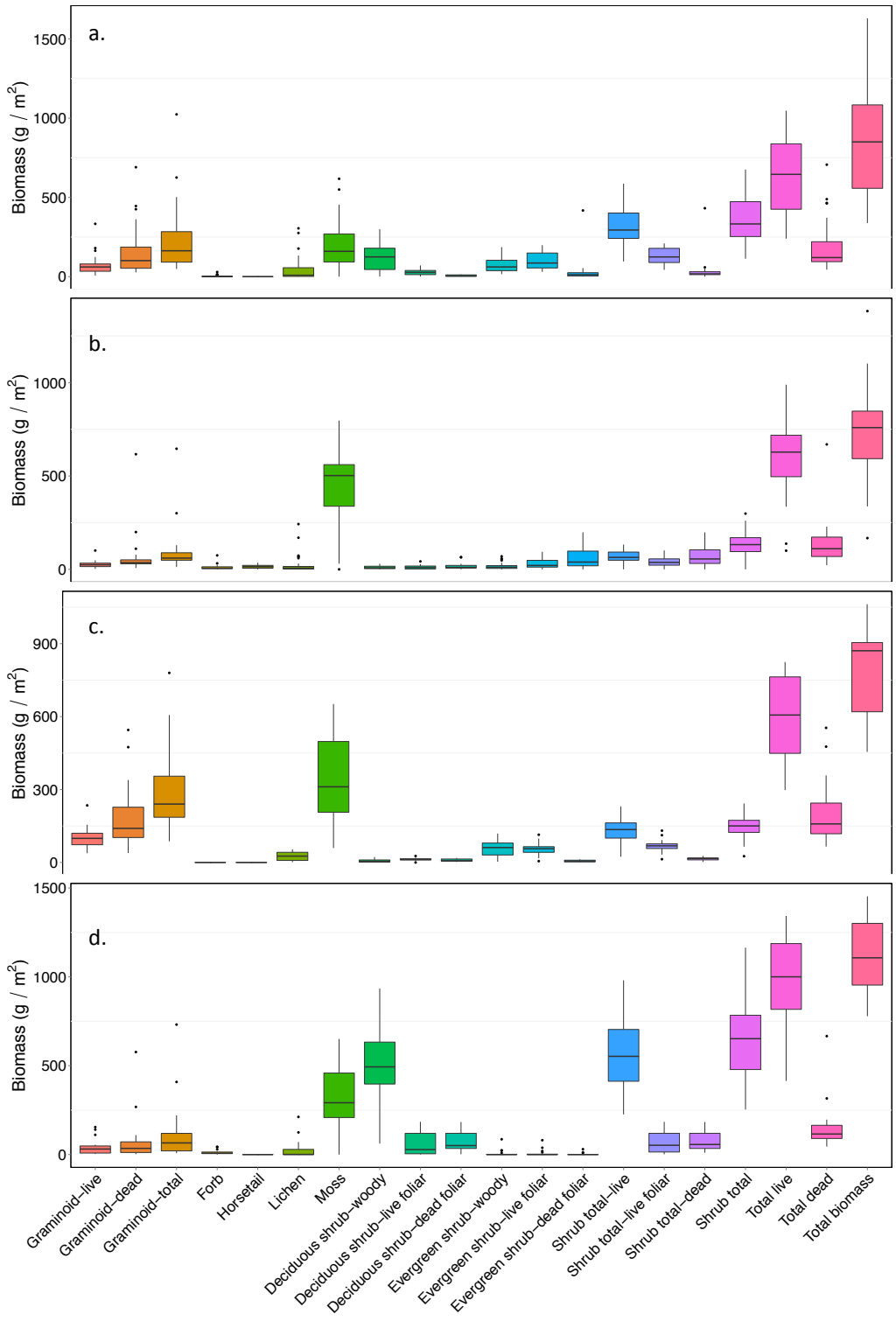

Figure 2.10. Biomass quantity per plant tissue type biomass component during peak growing season for the four vegetation communities of MAT (a), MNT (b), MT (c), ST (d) at Ivotuk, Alaska.

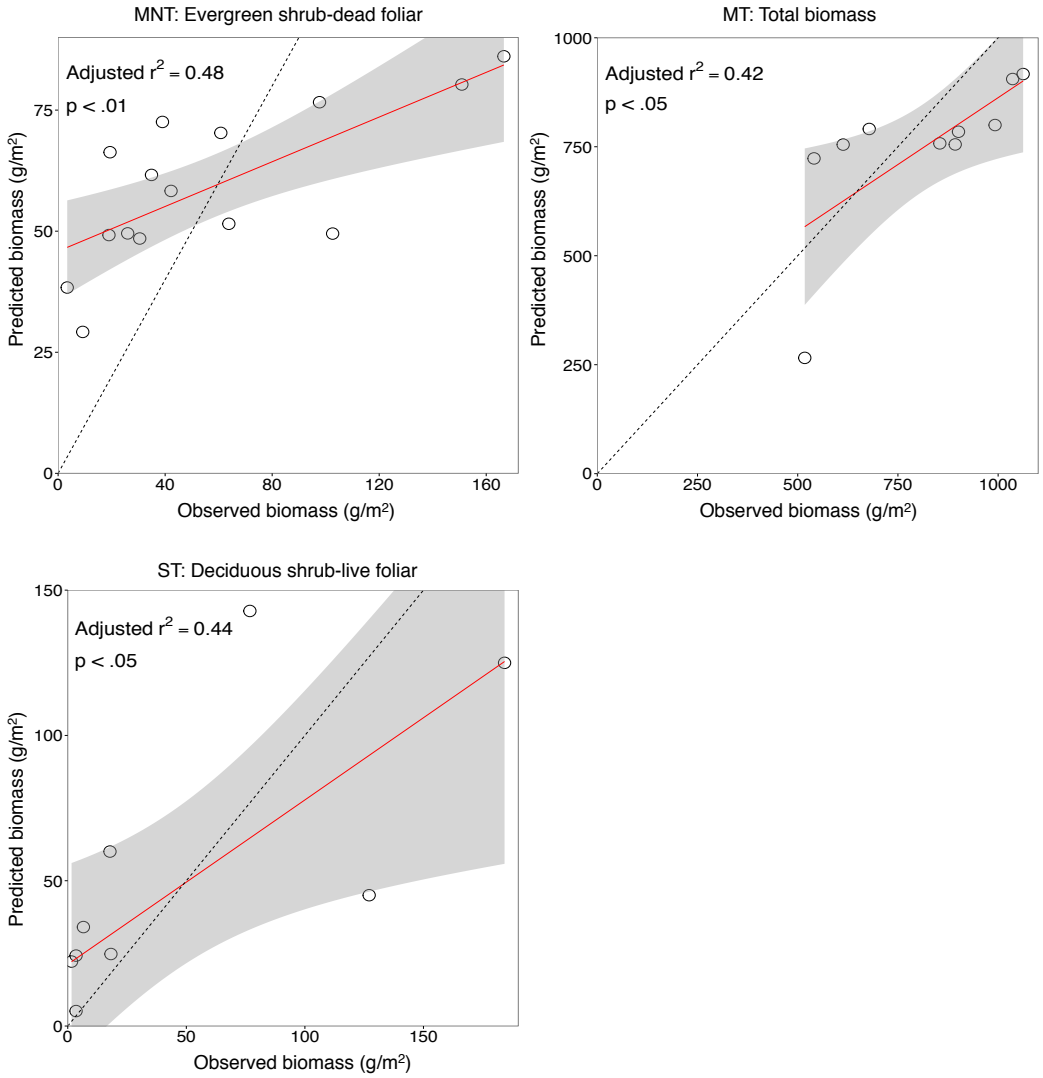

Figure 2.11. Relationship between plant tissue type biomass components for vegetation communities during peak growing season. Best relationships were for MNT and evergreen shrub-dead foliar, MT and grand total biomass, and ST and deciduous shrub-live foliar. The solid red line represents the best-fit line, and the dashed line is the 1:1 line.

Table 2.6. Significant relationships during peak growing season for four vegetation communities at Ivotuk, Alaska

Community	Plant Tissue Type	Predictor Bands	Adjusted r-square	p

MNT	Evergreen shrub-dead foliar	695	0.48	< .01
MNT	Shrub total-dead	400, 535, 540, 700	0.45	< .01
MT	Grand total	425, 430, 440, 570, 575, 680, 710, 715, 720, 940, 995, 1000	0.42	< .05
MT	Moss	425, 570, 710	0.36	< .05
ST	Deciduous shrub-live foliar	400, 410, 930, 1000	0.44	< .05

4.7 Spectra during peak growing season – without community separation

The majority of HNBs present in the biomass-spectra relationships for peak growing season and without separation by community type were in the near infrared wavelength and green wavelength regions (Figure 2.12). The next most common was the red edge, followed by the near infrared plateau, blue and red, and finally orange. In addition to being one of the dominant spectral regions, green wavelengths load more highly than most other segments. Blue also loads very highly, but is not one of the most common spectral regions in these relationships. Bands in the yellow, orange, red, and lower wavelengths of the near infrared also load more highly than longer wavelengths.

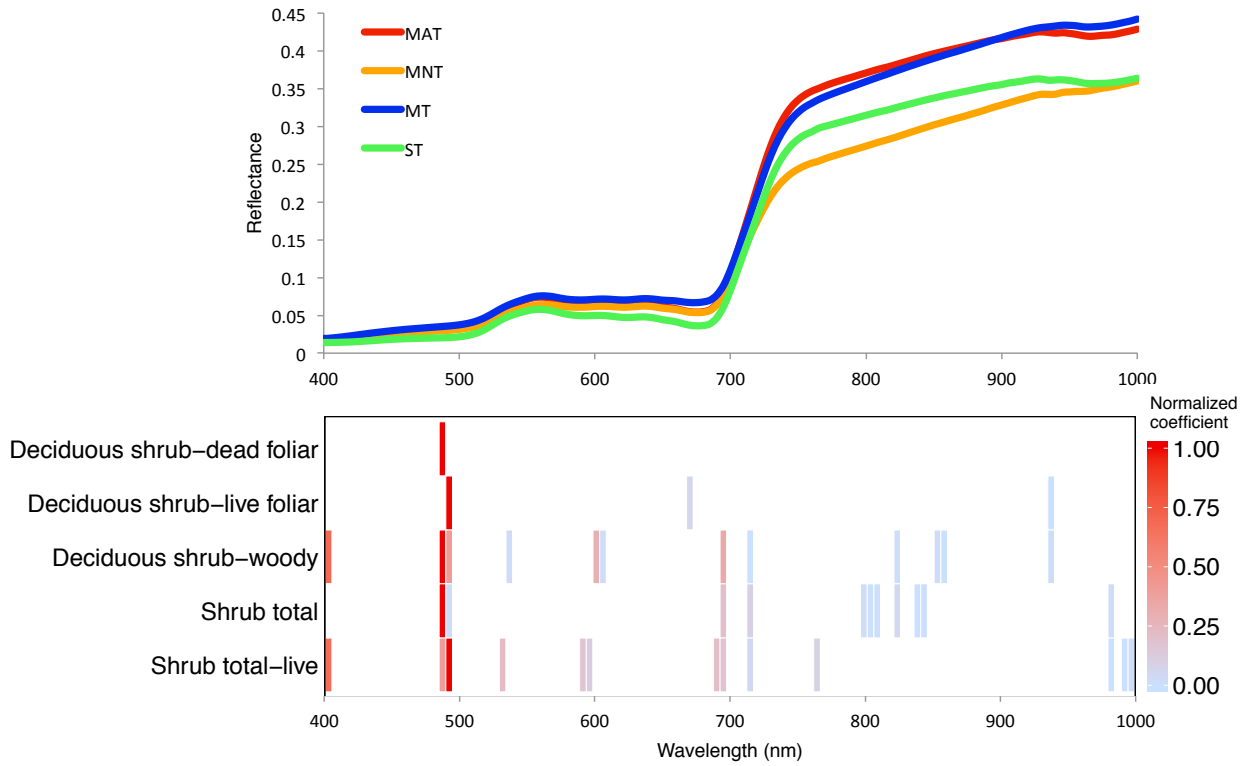

Figure 2.12. Mean reflectance for all vegetation communities during peak growing season along with the normalized coefficients for the optimal HNBs associated with the plant tissue type categories for total biomass.

4.8 Spectra during peak growing season – with community separation

The majority of HNBs for peak growing season with separation by vegetation community type were located in the red edge and blue regions (Figure 2.13). The next most common region was the near infrared plateau, followed by yellow and green. No bands in the orange, red, or NIR were used. Bands in the green and red edge were dominant in MNT, while bands in the red edge were dominant in MT. Bands in the blue and NIR plateau were equally dominant in ST. Bands in the blue, red edge, and green load most highly in MNT. Bands in the blue load most highly in MT, and bands in the blue load more highly than those in the near infrared plateau in ST.

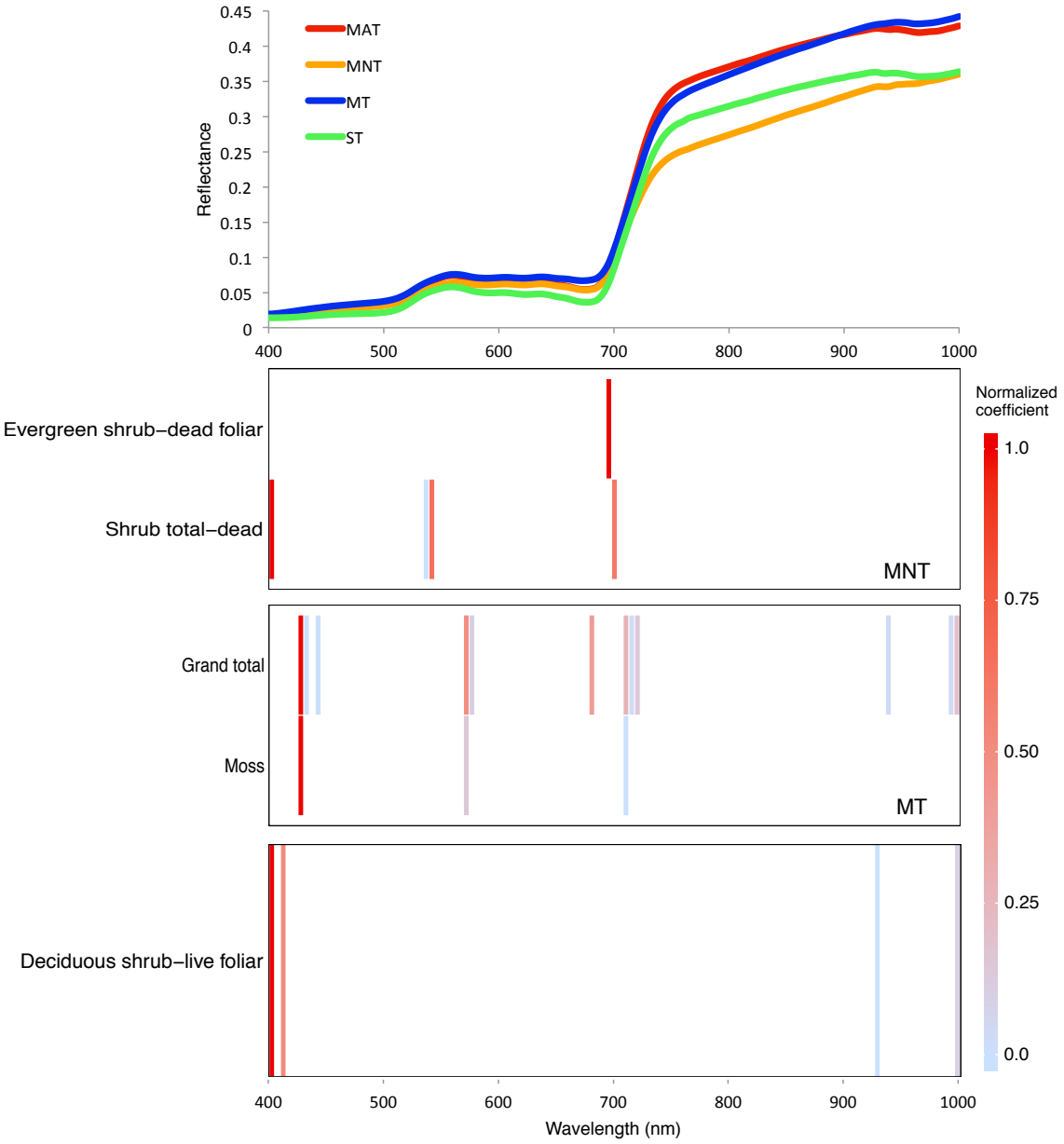

Figure 2.13. Mean reflectance for all vegetation communities during peak growing season along with the normalized coefficients for the optimal HNBs associated with the plant tissue type categories for biomass per vegetation communities.

5. Discussion

This study uses LASSO regression to identify relationships between biomass categories and significant wavelengths in four vegetation communities at Ivotuk, Alaska. Biomass-spectra relationships were established both with and without separation by vegetation community type. Results support the Riedel et al. (2005b) findings that shrubs are dominant controls over spectral reflectances at Ivotuk, as 65% of significant biomass-spectra relationships were for shrub or shrub component parts. However, these findings suggest that areas of the spectra outside the typical range of NDVI may be more useful for creating biomass-spectra relationships as bands in the blue, green, and red edge wavelengths loaded very highly for the majority of biomass-spectra relationships. These findings support results by Bratsch et al. (2016) (Chapter 1) indicating that state that bands outside typical NDVI ranges may be more useful for discriminating among vegetation community types than simply NDVI itself.

Mosses contributed the greatest amounts of biomass to vegetation communities at Ivotuk, Alaska. However, the majority of significant biomass-spectra relationships were for shrub vegetation at all times of the growing season. Past research has highlighted the importance of live foliar shrub materials as dominant controls over spectral reflectance in MAT and ST, but has noted that graminoids and bryophytes tend to dominate in MNT and MT (Riedel et al. 2005b). This research suggests that MAT, MNT, and MT all have spectral reflectances associated with shrub biomass. At peak growing season, MT is most closely associated with moss biomass, and is the only example of a significant moss-spectra relationship in this study. Therefore, although mosses comprise large quantities of vegetation biomass at Ivotuk, estimation of moss biomass remains problematic using hyperspectral remote sensing, an aspect potentially due to shading by overlying shrub vegetation.

There were twenty-six total significant relationships between plant tissue type biomass components and spectra at Ivotuk, Alaska. Seventeen significant relationships were for shrub or shrub component parts, six were for lower-lying plant tissue types such as dead biomass, graminoid, and moss, and three were for total categories. There were sixteen significant biomass-spectra relationships during early growing season but only ten during peak growing season.

Differences in composition of vascular and non-vascular vegetation determine many of the differences among vegetation communities in the Alaskan Arctic. Biomass-spectra relationships per individual community are stronger during early growing season, which may be attributable to the contribution of non-vascular plants to spectral signatures during the early growing season, perhaps when they are not being shaded by vascular vegetation. These results suggest that differences in biomass-spectra relationships are more apparent during early growing season, and decrease during peak growing season, resulting in a decreased ability to develop significant relationships between biomass and spectra during peak growing season at the individual community level. The problem with establishing biomass-spectra relationships for individual communities during peak growing season may be attributable to increased shrub cover during peak growing season, shading of non-vascular vegetation, similarities in species composition, and the masking of spectral information from underlying vegetation. These results suggest that community separation may be a better method for establishing biomass-hyperspectral relationships during early growing season, while analyses without community separation may be a better method during peak growing season.

Overall, hyperspectral bands associated with pigments (400-700nm) loaded highest when establishing biomass-spectra relationships without separation by vegetation community type during both early and peak growing season. Bands in the NIR that are associated with plant

structure were only significant for four relationships during early growing season with separation by vegetation community type. These relationships were for live and live foliar shrub components. Unlike (Bratsch et al. 2016) where vegetation structure becomes more important for community discrimination during peak growing season and reliance on NIR bands increase, in this study, the high loading of wavelengths in the green and blue remains consistent during all times of the growing season. This indicates a strong reliance on hyperspectral wavelengths associated with chlorophyll absorption during all parts of the growing season. In general, bands associated with chlorophyll, some of these located outside the typical range of broad-band NDVI, are the most significant for determining biomass quantities at Ivotuk, Alaska.

6. Conclusions

Arctic vegetation communities vary in plant species and plant functional type composition and biomass quantities. Along with physiological features in plant species, these differences result in spectral variations that are identifiable through hyperspectral remote sensing, and allow for the creation of biomass-spectra relationships. This study presents an example of the use of hyperspectral information for establishing these biomass-spectra relationships. This allows us to create remote ways of tracking increases in biomass quantities with climate change without incurring the large monetary and time cost traditionally associated with arctic research. The above research presents a method for developing biomass-spectral relationships using handheld hyperspectral data that can then be used to identify bands on upcoming satellite missions such as the NASA Hyperspectral Infrared Imager (HyspIRI) and the German Environmental Mapping and Analysis Program (EnMAP) that would be useful for tracking changes in vegetation biomass. Establishing these relationships at the ground level allows for the potential use of these methods to monitor changes to biomass occurring with increasing temperatures in the Arctic at much larger spatial and longer temporal extents.

7. References

Bhatt, U. S., D. A. Walker, M. K. Raynolds, J. C. Comiso, H. E. Epstein, G. Jia, R. Gens, J. E. Pinzon, C. J. Tucker, C. E. Tweedie, and P. J. Webber. 2010. Circumpolar Arctic Tundra Vegetation Change Is Linked to Sea Ice Decline. Earth Interactions **14**:1-20.

Bratsch, S., H. Epstein, M. Buchhorn, and D. Walker. 2016. Differentiating among Four Arctic Tundra Plant Communities at Ivotuk, Alaska Using Field Spectroscopy. Remote Sensing **8**:51.

Buchhorn, M., D. Walker, B. Heim, M. Raynolds, H. Epstein, and M. Schwieder. 2013. Ground-Based Hyperspectral Characterization of Alaska Tundra Vegetation along Environmental Gradients. Remote Sensing **5**:3971-4005.

CAVM. 2003. Circumpolar Arctic Vegetation Map. (1:7,500,000 scale), Conservation of Arctic Flora and Fauna (CAFF) Map No. 1. U.S. Fish and Wildlife Service, Anchorage, Alaska.

Chapin, F. S., G. R. Shaver, A. E. Giblin, K. J. Nadelhoffer, and J. A. Laundre. 1995. Responses of Arctic Tundra to Experimental and Observed Changes in Climate. Ecology **76**:694-711.

Comiso, J. C., and D. K. Hall. 2014. Climate trends in the Arctic as observed from space. Wiley Interdisciplinary Reviews: Climate Change **5**:389-409.

Cornelissen, J. H., T. V. Callaghan, J. M. Alatalo, A. Michelsen, E. Graglia, A. E. Hartley, D. Hik, S. E. Hobbie, M. C. Press, C. H. Robinson, G. H. Henry, G. R. Shaver, G. K. Phoenix, D. Gwynn Jones, S. Jonasson, F. S. Chapin III, U. Molau, C. Neill, J. A. Lee, J. M. Melillo, B. Sveinjörnsson, and R. Aerts. 2001. Global change and arctic ecosystems: is lichen decline a function of increases in vascular plant biomass? Journal of Ecology **89**:984-994.

Curran, P. J. 1989. Remote Sensing of Foliar Chemistry. Remote Sensing of Environment **30**:271-278.

DeMarco, J., M. C. Mack, and M. S. Bret-Harte. 2014. Effects of arctic shrub expansion on biophysical versus biogeochemical drivers of litter decomposition. Ecology.

Epstein, H. E., M. P. Calef, M. D. Walker, F. S. Chapin III, and A. M. Starfield. 2004. Detecting changes in arctic tundra plant communities in response to warming over decadal time scales. Global Change Biology **10**:1325-1334.

Epstein, H. E., M. K. Raynolds, D. A. Walker, U. S. Bhatt, C. J. Tucker, and J. E. Pinzon. 2012. Dynamics of aboveground phytomass of the circumpolar Arctic tundra during the past three decades. Environmental Research Letters **7**:015506.

Epstein, H. E., D. A. Walker, M. K. Raynolds, G. J. Jia, and A. M. Kelley. 2008. Phytomass patterns across a temperature gradient of the North American arctic tundra. Journal of Geophysical Research **113**.

Forbes, B. C., M. M. Fauria, and P. Zetterberg. 2010. Russian Arctic warming and 'greening' are closely tracked by tundra shrub willows. Global Change Biology **16**:1542-1554.

Friedman, J., T. Hastie, and R. Tibshirani. 2010. Regularization Paths for Generalized Linear Models via Coordinate Descent. Journal of Statistical Software **33**:1-22.

Hansen, J., R. Ruedy, M. Sato, and K. Lo. 2010. Global Surface Temperature Change. Reviews of Geophysics **48**.

Hobbie, S. E., A. Shevtsova, and F. S. Chapin III. 1999. Plant Responses to Species Removal and Experimental Warming in Alaskan Tussock Tundra. Oikos **84**:417-434.

Hope, A., J. S. Kimball, and D. Stow. 1993. The relationship between tussock tundra spectral reflectance properties and biomass and vegetation composition. International Journal of Remote Sensing **14**:1861-1874.

Huemmrich, F., J. A. Gamon, C. E. Tweedie, P. Campbell, D. R. Landis, and E. Middleton. 2013. Arctic Tundra Vegetation Functional Types Based on Photosynthetic Physiology and Optical Properties. IEEE Journal of Selected Topics in Applied Earth Observations and Remote Sensing **6**:265-275.

Huemmrich, K. F., G. Kinoshita, J. A. Gamon, S. Houston, H. Kwon, and W. C. Oechel. 2010. Tundra carbon balance under varying temperature and moisture regimes. Journal of Geophysical Research **115**.

Jia, G. J., H. E. Epstein, and D. Walker. 2002. Spatial characteristics of AVHRR-NDVI along latitudinal transectsin northern Alaska. Journal of Vegetation Science **13**:315-326.

Jia, G. J., H. E. Epstein, and D. A. Walker. 2004. Controls over intra-seasonal dynamics of AVHRR NDVI for the Arctic tundra in northern Alaska. International Journal of Remote Sensing **25**:1547-1564.

McGuire, A. D. 2003. Arctic Transitions in the Land–Atmosphere System (ATLAS): Background, objectives, results, and future directions. Journal of Geophysical Research **108**.

Muller, S. V., A. E. Racoviteanu, and D. A. Walker. 1999. Landsat MSS-derived land-cover map of northern Alaska: extrapolation methods and a comparison with photo-interpreted and AVHRR-derived maps. International Journal of Remote Sensing **20**:2921-2946.

Myers-Smith, I. H., B. C. Forbes, M. Wilmking, M. Hallinger, T. Lantz, D. Blok, K. D. Tape, M. Macias-Fauria, U. Sass-Klaassen, E. Lévesque, S. Boudreau, P. Ropars, L. Hermanutz, A. Trant, L. S. Collier, S. Weijers, J. Rozema, S. A. Rayback, N. M. Schmidt, G. Schaepman-Strub, S. Wipf, C. Rixen, C. B. Ménard, S. Venn, S. Goetz, L. Andreu-Hayles, S. Elmendorf, V. Ravolainen, J. Welker, P. Grogan, H. E. Epstein, and D. S. Hik. 2011. Shrub expansion in tundra ecosystems: dynamics, impacts and research priorities. Environmental Research Letters **6**:045509.

Raynolds, M. K., D. A. Walker, H. E. Epstein, J. E. Pinzon, and C. J. Tucker. 2012. A new estimate of tundra-biome phytomass from trans-Arctic field data and AVHRR NDVI. Remote Sensing Letters **3**:403-411.

Raynolds, M. K., D. A. Walker, and H. A. Maier. 2006. NDVI patterns and phytomass distribution in the circumpolar Arctic. Remote Sensing of Environment **102**:271-281.

Riedel, S., H. E. Epstein, D. A. Walker, D. L. Richardson, M. P. Calef, E. Edwards, and A. Moody. 2005a. Spatial and Temporal Heterogeneity of Vegetation Properties among Four Tundra Plant Communities at Ivotuk, Alaska, U. S. A. Arctic, Antarctic, and Alpine Research **37**:25-33.

Riedel, S. M., H. E. Epstein, and D. A. Walker. 2005b. Biotic controls over spectral reflectance of arctic tundra vegetation. International Journal of Remote Sensing **26**:2391-2405.

Serreze, M. C., and J. A. Francis. 2006. The Arctic Amplification Debate. Climatic Change **76**:241-264.

Silapaswan, C., D. Verbyla, and A. D. McGuire. 2001. Land Cover Change on the Seward Peninsula: The Use of Remote Sensing to Evaluate the Potential Influences of Climate Warming on Historical Vegetation Dynamics. Canadian Journal of Remote Sensing **27**:542-554.

Stow, D. A., A. Hope, D. McGuire, D. Verbyla, J. Gamon, F. Huemmrich, S. Houston, C. Racine, M. Sturm, K. Tape, L. Hinzman, K. Yoshikawa, C. Tweedie, B. Noyle, C. Silapaswan, D. Douglas, B. Griffith, G. Jia, H. Epstein, D. Walker, S. Daeschner, A. Petersen, L. Zhou, and R. Myneni. 2004. Remote sensing of vegetation and land-cover change in Arctic Tundra Ecosystems. Remote Sensing of Environment **89**:281-308.

Sturm, M., J. P. McFadden, G. E. Liston, F. S. Chapin III, C. Racine, and J. Holmgren. 2001. Snow-Shrub Interactions in Arctic Tundra: A Hypothesis with Climate Implications. Journal of Climate **14**:336-344.

Sturm, M., J. P. Schimel, G. J. Michaelson, J. M. Welker, S. F. Oberbauer, G. E. Liston, J. Fahnestock, and V. E. Romanovsky. 2005. Winter Biological Processes Could Help Convert Arctic Tundra to Shrubland. BioScience **55**:17-26.

Tenhunen, J. D., O. L. Lange, S. Hahn, R. Siegwolf, and S. F. Oberbauer. 1992. The Ecosystem Role of Poikilohydric Tundra Plants. Pages 213-239 *in* F. S. Chapin III, R. L. Jefferies, J. F. Reynolds, and G. R. Shaver, editors. Arctic Ecosystems in a Changing Climate: An Ecosphysiological Perspective. Academic Press, Inc., San Diego.

Tibshirani, R. 1996. Regression Shrinkage and Selection via the Lasso. Journal of the Royal Statistical Society. Series B (Methodological) **58**:267-288.

Ueyama, M., K. Iwata, Y. Harazono, E. S. Euskirchen, W. C. Oechel, and D. Zona. 2013. Growing season and spatial variations of carbon fluxes of Arctic and boreal ecosystems in Alaska (USA). Ecological Applications **23**:1798-1816.

Ustin, S. L., and J. A. Gamon. 2010. Remote sensing of plant functional types. New Phytol **186**:795-816.

van der Wal, R., and A. Stien. 2014. High arctic plants like it hot: a long-term investigation of between-year variability in plant biomass.

Walker, D., N. A. Auerbach, and M. Shippert. 1995. NDVI, biomass, and landscape evolution of glaciated terrain in northern Alaska. Polar Record **31**:169-178.

Walker, D., M. Raynolds, F. J. A. Daniels, E. Einarsson, A. Elvebakk, W. A. Gould, A. E. Katenin, S. S. Kholod, C. J. Markon, and B. A. Yurstev. 2005. The Circumpolar Arctic vegetation map. Journal of Vegetation Science **16**:267-282.

Walker, D. A. 1999. An integrated vegetation mapping approach for northern Alaska (1:4 M scale). International Journal of Remote Sensing **20**:2895-2920.

Walker, D. A. 2003. Phytomass, LAI, and NDVI in northern Alaska: Relationships to summer warmth, soil pH, plant functional types, and extrapolation to the circumpolar Arctic. Journal of Geophysical Research **108**.

Walker, D. A., H. E. Epstein, G. Jia, A. Balser, C. Copass, E. J. Edwards, W. A. Gould, J. Hollingsworth, J. A. Knudson, H. A. Maier, A. Moody, and M. K. Raynolds. 2003a. Phytomass, LAI, and NDVI in northern Alaska: Relationships to summer warmth, soil pH, plant functional types, and extrapolation to the circumpolar Arctic. Journal of Geophysical Research **108**.

Walker, D. A., H. E. Epstein, M. K. Raynolds, P. Kuss, M. A. Kopecky, G. V. Frost, F. J. A. Daniëls, M. O. Leibman, N. G. Moskalenko, G. V. Matyshak, O. V. Khitun, A. V. Khomutov, B. C. Forbes, U. S. Bhatt, A. N. Kade, C. M. Vonlanthen, and L. Tichý. 2012. Environment, vegetation and greenness (NDVI) along the North America and Eurasia Arctic transects. Environmental Research Letters **7**:015504.

Walker, D. A., G. J. Jia, H. E. Epstein, M. K. Raynolds, F. S. Chapin Iii, C. Copass, L. D. Hinzman, J. A. Knudson, H. A. Maier, G. J. Michaelson, F. Nelson, C. L. Ping, V. E.

Romanovsky, and N. Shiklomanov. 2003b. Vegetation-soil-thaw-depth relationships along a low-arctic bioclimate gradient, Alaska: synthesis of information from the ATLAS studies. Permafrost and Periglacial Processes **14**:103-123.

Walker, M. D., D. Walker, and N. A. Auerbach. 1994. Plant communities of a tussock tundra landscape in the Brooks Range Foothills, Alaska. Journal of Vegetation Science **5**:843-866.

Westhoff, V., and E. van der Meel. 1973. The Braun-Blanquet approach. Pages 617-726 *in* R. H. Whittaker, editor. Ordination and classification of communities. Dr. W. Junk, Den Haag, NL.

Winton, M. 2006. Amplified Arctic climate change: What does surface albedo feedback have to do with it? Geophysical Research Letters **33**.

Xu, H., T. Twine, and X. Yang. 2014. Evaluating Remotely Sensed Phenological Metrics in a Dynamic Ecosystem Model. Remote Sensing **6**:4660-4686.

Zeng, H., G. Jia, and H. Epstein. 2011. Recent changes in phenology over the northern high latitudes detected from multi-satellite data. Environmental Research Letters **6**:045508.

Chapter 3: Synthesis and Conclusions

This thesis investigates the utility of hyperspectral remote sensing data from the site of Ivotuk, Alaska for vegetation community discrimination and identification of biomass-spectra relationships. The Arctic has experienced significant warming trends over the past few decades, resulting in changes to albedo, heat fluxes, and temperature seasonality and associated changes to vegetation composition and increases in Low Arctic tundra vegetation biomass. Remote sensing is a valuable tool for tracking these changes, and establishing community-spectra and biomass-spectra relationships using handheld hyperspectral data is the first step toward developing methods that can be used to track vegetation changes on larger temporal and spatial scales. Normalized Difference Vegetation Index (NDVI) has historically been used to estimate vegetation biomass and community type, but many ecosystems are changing at the species level with minute differences that may not be identifiable using broad-band NDVI. Hyperspectral data is useful for filling in the gaps left by broad-band indices, and can be used to identify finer differences between arctic vegetation communities.

This study used hyperspectral data collected during the 1999 growing season from the primary study site of Ivotuk, Alaska, and five other sites along the North Slope of Alaska and the Brooks Mountain Range. In Chapter 1, I use hyperspectral bands and a two-step SPLS and LDA approach to differentiate among vegetation communities at Ivotuk, Alaska. This model is then applied to five other sites along the Dalton Highway in Alaska: Deadhorse, Franklin Bluffs, Sagwon-MNT, Sagwon-MAT, and Happy Valley. The results suggest that differentiation models can successfully be applied to other sites in the Alaskan Arctic with a caveat against latitudinal and regional differences in vegetation communities. Differentiation models from Ivotuk were most accurate within the site itself, and then next most accurate when applied to neighboring

sites in the Low Arctic including Happy Valley and Sagwon-MAT, but were less accurate when applied to more northern sites such as Deadhorse and Franklin Bluffs, which had the two lowest classification accuracies. This suggests that classification models would be best used within the confines of the same CAVM subzone, and that different models may be required for more northern subzones. Similarities in composition of vascular and non-vascular vegetation within vegetation communities still led to misclassification, with the most compositionally similar vegetation types of MAT and ST as the most commonly misclassified in this study. The most significant bands for community discrimination were located outside of the typical regions of broad-band NDVI. Bands associated with pigments (400-700 nm) loaded the highest during early growing season and structural tissue (NIR) loaded the highest during peak growing season. Discriminability for the Dalton Highway sites relied heavily on bands in the red edge (680-725 nm). Although NIR values were significant, they were never used in a model that also used red wavelengths.

In Chapter 2, I use LASSO regression analysis to develop biomass-spectra relationships and estimate biomass quantities at Ivotuk, Alaska. Biomass-spectra relationships were developed with and without separation by vegetation community type. Once again, these findings support that shrubs are dominant controls over spectral reflectance in the Artic as the majority of significant biomass-spectra relationships were for shrubs or shrub component parts. While mosses contribute the largest quantities of biomass to vegetation communities, shrubs had more significant biomass-spectra relationships, perhaps owing to the shading of mosses by shrubs. Findings again suggest that spectral regions outside of NDVI including the blue, green, and red edge are better for estimating biomass in Low Arctic tundra vegetation communities. Bands in the 400-700 nm range were most significant during all times of the growing season, unlike

Chapter 1, where structural bands (NIR) were more important during peak growing season. Although mosses comprise the largest quantities of vegetation biomass, we may only be able to properly assess overlying shrub biomass using hyperspectral remote sensing, especially during peak growing season. This suggests that community differences in vegetation biomass may best be assessed during early growing season.

This research is an example of the benefits of using hyperspectral remote sensing to differentiate among vegetation communities and estimate biomass in the Alaskan Arctic. Hyperspectral remote sensing allows us to better capture minute differences in vegetation communities that might otherwise be obscured with broad-band remote sensing methods such as NDVI. Both chapters in this thesis seek to identify narrow spectral regions that can be used to accomplish these tasks, and highlight the importance of hyperspectral narrowbands in the blue, green, and red edge regions of the spectra. Arctic vegetation communities are changing over large spatial scales as temperatures increase. Monitoring these changes through hyperspectral remote sensing would allow us to better track the minute species-level changes occurring in vegetation communities. Establishing relationships using ground-based studies such as this is essential to the process of developing biomass-spectra and community-spectra relationships that can be scaled to hyperspectral remote sensing satellite platforms and used to track and understand vegetation changes occurring with climate change at broader spatial and temporal scales.